Figure 4. siRNA knock down of AGO2 expression. A) Knock down of *AGO2* expression in T23 cells by specific siRNAs for *AGO2* or control siRNAs, confirmed by real-time quantitative RT-PCR analysis. B) Supernatant HBs antigen, and C) HBV-DNA were measured. Both were higher in supernatant of cells transfected with si-control than in cells transfected with si-*AGO2*. D) There was no significant difference in cell viability between cells transfected with si-control compared to those with si-*AGO2*.
doi:10.1371/journal.pone.0047490.g004

controls. Mir-122, miR-22, miR-99a, and miR-125b in particular, were significantly elevated in serum of HBV patients. We also showed that AGO2, an essential component of the RNA silencing complex, co-localizes with both HBc and HBs proteins. HBc and/or HBs localize to several organelles associated with protein synthesis, processing, and degradation, including the ER, Golgi, endosomes, autophagosomes, processing bodies, and multivesicular bodies. Although we expected that depletion of AGO2 would relieve inhibition of HBV replication, we found instead that knockdown of AGO2 appears to inhibit HBV replication, implying that HBV may require AGO2 during its life cycle.

The role of AGO2 is unclear, but viruses have previously been shown to interfere with elements of the RNA-induced gene silencing pathway [17]. HCV core protein and the HIV-1 Tat protein suppress gene silencing by inhibiting Dicer, a cytoplasmic protein that processes pre-microRNA [18]. HBV down-regulates expression of Drosha, the nuclear protein involved in the first step of miRNA processing, which might globally suppress miRNA expression levels [19]. Viruses also influence expression of individual miRNAs [17].

Considering that miR-122 strongly suppresses HBV replication, it is curious that HBV is nonetheless often able to establish chronic infection in the liver [20,21,22]. In the case of HCV, miR-122/AGO2 binding stabilizes the HCV genome and prevents degradation, such that suppression of either miR-122 or AGO2 inhibits HCV replication [23,24,25]. In HBV, we also found that AGO2 knockdown suppresses replication, but Wang et al. demonstrated that anti-sense depletion of miR-122 promoted HBV replication instead of suppressing it [26]. MiR-122 suppresses HBV replication both through direct binding to HBV RNA as well as indirectly through cyclin G1-modulated p53 activity [20,27,28]. HBV might therefore be expected to down-regulate miR-122 levels to evade miR-122 binding and suppression. Wang et al. indeed found that miR-122 levels are significantly decreased in the liver of chronic HBV patient [26], whereas elevated miR-122 levels in the serum have been reported [4,29].

One explanation for the discrepancy between liver and serum miR-122 levels might be that HBV sequesters and expels AGO2-bound miR-122 inside of HBsAg particles, possibly along with other miRNAs that interfere with the viral life cycle. HBV vastly over-produces surface proteins that self-assemble into what were initially thought to be empty particles [30,31], but which may contain miRNAs stably bound to AGO2 [5]. Although HBV is a DNA virus, it relies on reverse transcription via an RNA intermediate in a way similar to retroviruses. Bouttier et al. showed that two unrelated retroviruses, HIV-1 and PFV-1, both require AGO2 interaction with viral RNA for assembly of viral particles. In these viruses, AGO2 is recruited to viral RNA and encapsidated along with it without impairing translation of viral RNA [32]. This suggests that some viruses may take advantage of another function of Argonaute, such as its role in the formation of P-bodies [33], although AGO2 possesses intrinsic exonuclease activity that must be countered. AGO2-mediated gene silencing requires recruitment of GW182 via multiple GW-rich regions [34]. While HIV-1 and PFV-1 encapsidate AGO2, they do not encapsidate GW182, which might provide a means to suppress AGO2 silencing. Some plant viruses use molecular mimicry to inhibit RISC activity by binding to Argonaute proteins through virally encoded WG/GW motifs [35]. Although HBV proteins appear to lack WG/GW motifs, the HBV core protein may use a similar mechanism to disrupt RISC activity while preserving other AGO2 functions. One possibility involves HSP90, a chaperone involved in maintenance of the polymerase/pgRNA complex. HSP90 binds to HBV core protein dimers and is internalized in capsids, but it also binds to the N-terminus of AGO2 and may be required for miRNA loading and targeting to P-bodies [36,37]. Co-localization studies with other proteins and analysis of bound miRNAs may be necessary to elucidate the role of AGO2 in HBV replication, but we speculate that HBV proteins might suppress miRNA activity by binding to and sequestering AGO2 and their bound miRNAs.

Pathway analysis of the predicted targets of the up-regulated serum miRNAs in HBV patients showed that genes involved in phosphatase activity were significantly over-represented. Each of several miRNAs, including miR-122, miR-125b, and miR-99a, was predicted to target a different phosphorylation-associated gene. Regulation of phosphorylation appears to be important in HBV replication, as phosphorylation of the C terminal domain of the HBV core protein is essential for pgRNA packaging and HBV capsid maturation [38]. Phosphorylation also inhibits AGO2 binding of miRNA [39] and is involved in localization to P-bodies [40]. Recent studies have demonstrated that HBV enhances and exploits autophagy via the HBx and small HBs proteins to promote viral DNA replication and envelopment without increasing the rate of protein degradation [41,42]. Sir et al suggested that autophagy may affect dephosphorylation and maturation of the core protein, which protects viral DNA during replication [43]. These reports suggest that HBV exploits multiple cellular pathways in order to establish an intracellular environment conducive to replication.

Although many HBV-associated miRNAs have been reported, the functions of only a few have been examined. MiR-122, miR-125a-5p, miR-199a-3p and miRNA-210 have all been reported to bind to and directly suppress HBV RNA [8,27,44], whereas other miRNAs have been shown to promote or suppress HBV replication indirectly. MiR-1 enhances HBV core promoter activity by up-regulating FXRα, a transcription factor essential for HBV replication [45], whereas miR-141 suppresses HBsAg production in HepG2 cells by down-regulating promoter activity via PPARA [46]. The role of miR-22 and miR-99a in HBV infection is less clear, but both are involved in regulation of cell fate and are implicated in development of HCC. MiR-99a is one of the most highly expressed miRNAs in normal liver tissue and is severely down-regulated in HCC and other cancers, suggesting a role as a tumor suppressor [47]. MiR-99a alters sensitivity to TGF-β activity by suppressing phosphorylation of SMAD3 [48], whereas the HBx protein disrupts TGF-β signaling by shifting from the pSmad3C pathway to the oncogenic pSmad3L pathway [49]. MiR-22 acts as a tumor suppressor by inducing cellular senescence and is down-regulated in several cancer lines [50]. However, over-expression of miR-22 in males is associated with down-regulation of ERα expression, which compromises the protective effect of estrogen and leads to up-regulation of IL-1α in hepatocytes under stress caused by reactive oxygen species, which is another hallmark of HBx interference [51]. Differences in

miRNA levels between hepatic and serum miRNA profiles may reveal miRNAs that play an essential role in the HBV life cycle, with potential application to miRNA-based diagnosis and therapy.

In this study we demonstrated potential interactions between AGO2 and HBc and HBs, but not HBx, in stably transfected HepG2 cells. Suppression of HBV DNA and HBsAg in the supernatant following AGO2 knockdown and the presence of HBV-associated miRNAs in the serum may indicate a dependency on AGO2 during the HBV life cycle.

Supporting Information

Figure S1 Heat map of miRNA expression. Healthy controls and patients with chronic HBV clustered separately based on serum miRNA expression. "Healthy males" and "healthy females" refer to serum mixtures of 12 uninfected males and 10 uninfected females, respectively. "HBV low" and "HBV high" refer to serum mixtures from 10 patients with low (≤42 IU/l) ALT levels and 10 patients with high ALT levels (>42 IU/l), respectively.
(TIF)

Figure S2 Pairwise correlations among pooled serum miRNA samples. Pooled serum samples were collected from 10 healthy males, 10 healthy females, 10 HBV patients with low ALT levels, and 10 HBV patients with high ALT levels. Pairwise correlations in miRNA expression levels among all four pooled samples were strong (>0.90; P<0.001), but correlations were strongest between the healthy male and female samples (0.98) and between the low and high ALT HBV patients (0.98), suggesting that expression of a subset of miRNAs is altered during HBV infection.
(TIF)

Figure S3 Relationship between serum miRNAs and HBsAg levels in chronic HBV patients. Serum levels of several miRNAs were significantly correlated with HBsAg levels in patients with chronic HBV. MiR-99a, miR-122, and miR-125b levels were most strongly correlated with HBsAg levels, with R^2 of 0.69, 0.56, and 0.54, respectively.
(TIF)

Figure S4 Relationship between serum miRNAs and HBV DNA levels in chronic HBV patients. Serum levels of several miRNAs were significantly correlated with HBV DNA levels in patients with chronic HBV. MiR-122, miR-99a, and miR-125b levels were most strongly correlated with HBV DNA levels, with R^2 of 0.44, 0.43, and 0.39, respectively.
(TIF)

Figure S5 Relationship between serum miRNAs and ALT levels in chronic HBV patients. Serum levels of several miRNAs were significantly but somewhat diffusely correlated with ALT levels in patients with chronic HBV. MiR-122 and miR-22 levels were correlated with ALT levels with R^2 of 0.25 and 0.21, respectively.
(TIF)

Figure S6 Relationship between serum miRNAs and presence of HBe antigen in chronic HBV patients. Serum levels of miR-122, miR-99a, miR-720, and miR-125b were significantly elevated in patients positive for the HBe antigen.
(TIF)

Figure S7 Relationship between serum miRNAs and presence of HBe antibody in chronic HBV patients. Serum levels of miR-122, miR-99a, miR-720, and miR-125b were significantly elevated in patients negative for the HBe antibody.
(TIF)

Figure S8 Relationship between individual miRNAs in the liver and serum. Each point represents the level of a specific miRNA in non-cancerous liver tissue relative to serum in the same patient. Red points represent miRNA levels from a patient with chronic HBV, and blue and green points correspond to two different uninfected control subjects. Large red points and labels indicate the subset of miRNAs (Tables 2 and 3) that were significantly elevated in serum of chronic HBV patients. MiRNA expression levels were positively correlated ($R^2 = 0.57$; P<2.1E-16) between liver tissue and serum, suggesting that serum levels broadly reflect miRNA levels in the liver. There appears to be no clear discrepancy between liver and serum miRNA levels in the HBV-infected patient compared to the two uninfected patients.
(TIF)

Figure S9 Subcellular localization of HBx analyzed by immunocytochemistry. HBx localized non-specifically in the nucleus and cytoplasm, but we were unable to verify the subcellular location. Anti-Rab5 staining for endosomes is shown for illustration, but results were similar using antibodies against other compartments.
(TIF)

Table S1 Antibodies used for immunocytochemistry.
(DOC)

Table S2 Significantly up- or down-regulated miRNAs in liver samples from an HBV-infected patient compared to two non-HBV-infected patients.
(DOC)

Acknowledgments

This work was carried out at the Analysis Center of Life Science, Hiroshima University.

Author Contributions

Conceived and designed the experiments: KC CNH SA MT DM HAB HO NH. Performed the experiments: MT DM H. Abe NH MI SY H. Aikata TK YK RA KC. Analyzed the data: CNH SA MT DM HO KC. Contributed reagents/materials/analysis tools: CNH SA MT DM KC. Wrote the paper: CNH SA MT DM KC. Clinical data: KC MT DM HAB NH MI ST HAI TK YK WO. Obtained funding: KC MT DM. Critical review of the manuscript: CNH SA MT DM RA HAB HO NH MI ST HAI TK YK WO KC.

References

1. Fields BN, Knipe DM, Howley PM (2007) Fields virology. Philadelphia: Wolters Kluwer Health/Lippincott Williams & Wilkins.
2. McMahon BJ (2009) The natural history of chronic hepatitis B virus infection. Hepatology 49: S45–55.
3. Brechot C, Kremsdorf D, Soussan P, Pineau P, Dejean A, et al. (2010) Hepatitis B virus (HBV)-related hepatocellular carcinoma (HCC): molecular mechanisms and novel paradigms. Pathologie-biologie 58: 278–287.
4. Ji F, Yang B, Peng X, Ding H, You H, et al. (2011) Circulating microRNAs in hepatitis B virus-infected patients. Journal of viral hepatitis 18: e242–251.
5. Novellino L, Rossi RL, Bonino F, Cavallone D, Abrignani S, et al. (2012) Circulating Hepatitis B Surface Antigen Particles Carry Hepatocellular microRNAs. PloS one 7: e31952.
6. Qi P, Cheng SQ, Wang H, Li N, Chen YF, et al. (2011) Serum MicroRNAs as Biomarkers for Hepatocellular Carcinoma in Chinese Patients with Chronic Hepatitis B Virus Infection. PloS one 6: e28486.
7. Ura S, Honda M, Yamashita T, Ueda T, Takatori H, et al. (2009) Differential microRNA expression between hepatitis B and hepatitis C leading disease progression to hepatocellular carcinoma. Hepatology 49: 1098–1112.

8. Zhang GL, Li YX, Zheng SQ, Liu M, Li X, et al. (2010) Suppression of hepatitis B virus replication by microRNA-199a-3p and microRNA-210. Antiviral research 88: 169–175.
9. Chen Y, Cheng G, Mahato RI (2008) RNAi for treating hepatitis B viral infection. Pharmaceutical research 25: 72–86.
10. Xi Y, Nakajima G, Gavin E, Morris CG, Kudo K, et al. (2007) Systematic analysis of microRNA expression of RNA extracted from fresh frozen and formalin-fixed paraffin-embedded samples. RNA 13: 1668–1674.
11. Turchinovich A, Weiz L, Langheinz A, Burwinkel B (2011) Characterization of extracellular circulating microRNA. Nucleic acids research 39: 7223–7233.
12. Liu AM, Zhang C, Burchard J, Fan ST, Wong KF, et al. (2011) Global regulation on microRNA in hepatitis B virus-associated hepatocellular carcinoma. Omics : a journal of integrative biology 15: 187–191.
13. Bala S, Marcos M, Szabo G (2009) Emerging role of microRNAs in liver diseases. World journal of gastroenterology : WJG 15: 5633–5640.
14. Desmet VJ, Gerber M, Hoofnagle JH, Manns M, Scheuer PJ (1994) Classification of chronic hepatitis: diagnosis, grading and staging. Hepatology 19: 1513–1520.
15. Tsuge M, Hiraga N, Takaishi H, Noguchi C, Oga H, et al. (2005) Infection of human hepatocyte chimeric mouse with genetically engineered hepatitis B virus. Hepatology 42: 1046–1054.
16. Weibrecht I, Leuchowius KJ, Clausson CM, Conze T, Jarvius M, et al. (2010) Proximity ligation assays: a recent addition to the proteomics toolbox. Expert review of proteomics 7: 401–409.
17. Cullen BR (2011) Viruses and microRNAs: RISCy interactions with serious consequences. Genes & development 25: 1881–1894.
18. Wang Y, Kato N, Jazag A, Dharel N, Otsuka M, et al. (2006) Hepatitis C virus core protein is a potent inhibitor of RNA silencing-based antiviral response. Gastroenterology 130: 883–892.
19. Ren M, Qin D, Li K, Qu J, Wang L, et al. (2012) Correlation between hepatitis B virus protein and microRNA processor Drosha in cells expressing HBV. Antiviral research.
20. Wang S, Qiu L, Yan X, Jin W, Wang Y, et al. (2011) Loss of MiR-122 expression in patients with hepatitis B enhances hepatitis B virus replication through cyclin G1 modulated P53 activity. Hepatology 55: 730–741.
21. Hu J, Xu Y, Hao J, Wang S, Li C, et al. (2012) MiR-122 in hepatic function and liver diseases. Protein & cell 3: 364–371.
22. Chang J, Nicolas E, Marks D, Sander C, Lerro A, et al. (2004) miR-122, a mammalian liver-specific microRNA, is processed from hcr mRNA and may downregulate the high affinity cationic amino acid transporter CAT-1. RNA biology 1: 106–113.
23. Narbus CM, Israelow B, Sourisseau M, Michta ML, Hopcraft SE, et al. (2011) HepG2 cells expressing microRNA miR-122 support the entire hepatitis C virus life cycle. Journal of virology 85: 12087–12092.
24. Shimakami T, Yamane D, Jangra RK, Kempf BJ, Spaniel C, et al. (2012) Stabilization of hepatitis C virus RNA by an Ago2-miR-122 complex. Proceedings of the National Academy of Sciences of the United States of America 109: 941–946.
25. Wilson JA, Zhang C, Huys A, Richardson CD (2011) Human Ago2 is required for efficient microRNA 122 regulation of hepatitis C virus RNA accumulation and translation. Journal of virology 85: 2342–2350.
26. Wang S, Qiu L, Yan X, Jin W, Wang Y, et al. (2012) Loss of microRNA 122 expression in patients with hepatitis B enhances hepatitis B virus replication through cyclin G(1) -modulated P53 activity. Hepatology 55: 730–741.
27. Chen Y, Shen A, Rider PJ, Yu Y, Wu K, et al. (2011) A liver-specific microRNA binds to a highly conserved RNA sequence of hepatitis B virus and negatively regulates viral gene expression and replication. The FASEB journal : official publication of the Federation of American Societies for Experimental Biology 25: 4511–4521.
28. Qiu L, Fan H, Jin W, Zhao B, Wang Y, et al. (2010) miR-122-induced down-regulation of HO-1 negatively affects miR-122-mediated suppression of HBV. Biochemical and biophysical research communications 398: 771–777.
29. Waidmann O, Bihrer V, Pleli T, Farnik H, Berger A, et al. (2012) Serum microRNA-122 levels in different groups of patients with chronic hepatitis B virus infection. Journal of viral hepatitis 19: e58–65.
30. Heermann KH, Goldmann U, Schwartz W, Seyffarth T, Baumgarten H, et al. (1984) Large surface proteins of hepatitis B virus containing the pre-s sequence. Journal of virology 52: 396–402.
31. Patient R, Hourioux C, Sizaret PY, Trassard S, Sureau C, et al. (2007) Hepatitis B virus subviral envelope particle morphogenesis and intracellular trafficking. Journal of virology 81: 3842–3851.
32. Bouttier M, Saumet A, Peter M, Courgnaud V, Schmidt U, et al. (2012) Retroviral GAG proteins recruit AGO2 on viral RNAs without affecting RNA accumulation and translation. Nucleic acids research 40: 775–786.
33. Eulalio A, Behm-Ansmant I, Schweizer D, Izaurralde E (2007) P-body formation is a consequence, not the cause, of RNA-mediated gene silencing. Molecular and cellular biology 27: 3970–3981.
34. Lian SL, Li S, Abadal GX, Pauley BA, Fritzler MJ, et al. (2009) The C-terminal half of human Ago2 binds to multiple GW-rich regions of GW182 and requires GW182 to mediate silencing. RNA 15: 804–813.
35. Giner A, Lakatos L, Garcia-Chapa M, Lopez-Moya JJ, Burgyan J (2010) Viral protein inhibits RISC activity by argonaute binding through conserved WG/GW motifs. PLoS pathogens 6: e1000996.
36. Johnston M, Geoffroy MC, Sobala A, Hay R, Hutvagner G (2010) HSP90 protein stabilizes unloaded argonaute complexes and microscopic P-bodies in human cells. Molecular biology of the cell 21: 1462–1469.
37. Pare JM, Tahbaz N, Lopez-Orozco J, LaPointe P, Lasko P, et al. (2009) Hsp90 regulates the function of argonaute 2 and its recruitment to stress granules and P-bodies. Molecular biology of the cell 20: 3273–3284.
38. Lan YT, Li J, Liao W, Ou J (1999) Roles of the three major phosphorylation sites of hepatitis B virus core protein in viral replication. Virology 259: 342–348.
39. Rudel S, Wang Y, Lenobel R, Korner R, Hsiao HH, et al. (2011) Phosphorylation of human Argonaute proteins affects small RNA binding. Nucleic acids research 39: 2330–2343.
40. Zeng Y, Sankala H, Zhang X, Graves PR (2008) Phosphorylation of Argonaute 2 at serine-387 facilitates its localization to processing bodies. The Biochemical journal 413: 429–436.
41. Sir D, Tian Y, Chen WL, Ann DK, Yen TS, et al. (2010) The early autophagic pathway is activated by hepatitis B virus and required for viral DNA replication. Proceedings of the National Academy of Sciences of the United States of America 107: 4383–4388.
42. Li J, Liu Y, Wang Z, Liu K, Wang Y, et al. (2011) Subversion of cellular autophagy machinery by hepatitis B virus for viral envelopment. Journal of virology 85: 6319–6333.
43. Sir D, Ann DK, Ou JH (2010) Autophagy by hepatitis B virus and for hepatitis B virus. Autophagy 6.
44. Potenza N, Papa U, Mosca N, Zerbini F, Nobile V, et al. (2011) Human microRNA hsa-miR-125a-5p interferes with expression of hepatitis B virus surface antigen. Nucleic acids research 39: 5157–5163.
45. Zhang X, Zhang E, Ma Z, Pei R, Jiang M, et al. (2011) Modulation of hepatitis B virus replication and hepatocyte differentiation by MicroRNA-1. Hepatology 53: 1476–1485.
46. Hu W, Wang X, Ding X, Li Y, Zhang X, et al. (2012) MicroRNA-141 Represses HBV Replication by Targeting PPARA. PloS one 7: e34165.
47. Li D, Liu X, Lin L, Hou J, Li N, et al. (2011) MicroRNA-99a inhibits hepatocellular carcinoma growth and correlates with prognosis of patients with hepatocellular carcinoma. The Journal of biological chemistry 286: 36677–36685.
48. Turcatel G, Rubin N, El-Hashash A, Warburton D (2012) MIR-99a and MIR-99b modulate TGF-beta induced epithelial to mesenchymal plasticity in normal murine mammary gland cells. PloS one 7: e31032.
49. Murata M, Matsuzaki K, Yoshida K, Sekimoto G, Tahashi Y, et al. (2009) Hepatitis B virus X protein shifts human hepatic transforming growth factor (TGF)-beta signaling from tumor suppression to oncogenesis in early chronic hepatitis B. Hepatology 49: 1203–1217.
50. Xu D, Takeshita F, Hino Y, Fukunaga S, Kudo Y, et al. (2011) miR-22 represses cancer progression by inducing cellular senescence. The Journal of cell biology 193: 409–424.
51. Jiang R, Deng L, Zhao L, Li X, Zhang F, et al. (2011) miR-22 promotes HBV-related hepatocellular carcinoma development in males. Clinical cancer research: an official journal of the American Association for Cancer Research 17: 5593–5603.

HEPATOLOGY
Official Journal of the American Association for the Study of Liver Diseases

Severe Necroinflammatory Reaction Caused by Natural Killer Cell-Mediated Fas/Fas Ligand Interaction and Dendritic Cells in Human Hepatocyte Chimeric Mouse

Akihito Okazaki,[1,2] Nobuhiko Hiraga,[1,2] Michio Imamura,[1,2] C. Nelson Hayes,[1,2,3] Masataka Tsuge,[1,2] Shoichi Takahashi,[1,2] Hiroshi Aikata,[1,2] Hiromi Abe,[1,2,3] Daiki Miki,[1,2,3] Hidenori Ochi,[1,2,3] Chise Tateno,[2,4] Katsutoshi Yoshizato,[2,4] Hideki Ohdan,[2,5] and Kazuaki Chayama[1,2,3]

The necroinflammatory reaction plays a central role in hepatitis B virus (HBV) elimination. Cluster of differentiation (CD)8-positive cytotoxic T lymphocytes (CTLs) are thought to be a main player in the elimination of infected cells, and a recent report suggests that natural killer (NK) cells also play an important role. Here, we demonstrate the elimination of HBV-infected hepatocytes by NK cells and dendritic cells (DCs) using urokinase-type plasminogen activator/severe combined immunodeficiency mice, in which the livers were highly repopulated with human hepatocytes. After establishing HBV infection, we injected human peripheral blood mononuclear cells (PBMCs) into the mice and analyzed liver pathology and infiltrating human immune cells with flow cytometry. Severe hepatocyte degeneration was observed only in HBV-infected mice transplanted with human PBMCs. We provide the first direct evidence that massive liver cell death can be caused by Fas/Fas ligand (FasL) interaction provided by NK cells activated by DCs. Treatment of mice with anti-Fas antibody completely prevented severe hepatocyte degeneration. Furthermore, severe hepatocyte death can be prevented by depletion of DCs, whereas depletion of CD8-positive CTLs did not disturb the development of massive liver cell apoptosis. ***Conclusion:*** **Our findings provide the first direct evidence that DC-activated NK cells induce massive HBV-infected hepatocyte degeneration through the Fas/FasL system and may indicate new therapeutic implications for acute severe/fulminant hepatitis B.** (HEPATOLOGY 2012;56:555-566)

Between 4% and 32% of fulminant hepatitis cases, characterized by acute massive hepatocyte degeneration and subsequent development of hepatic encephalopathy and liver failure, are caused by acute hepatitis B virus (HBV) infection.[1] Host[2] and viral factors[3] may influence the development of fulminant hepatitis, but these factors have not been fully elucidated.

Innate and adaptive immunity both play a role in the elimination of viral infections. In the innate immune response, cytoplasmic and membrane-bound receptors recognize viruses and induce interferon (IFN)-β production, which, in turn, up-regulates IFN-α and induces an antiviral state in surrounding cells.[4] In the adaptive immune response, viruses are recognized by dendritic cells (DCs), which activate cluster of differentiation (CD)8-positive T cells to reduce viral replication through cytolytic[5] and noncytolytic mechanisms.[6] The role of immune cells, especially HBV-specific cytotoxic T lymphocytes (CTLs), is crucial in the

Abbreviations: APC, allophycocyanin; asialo GM1, ganglio-N-tetraosylceramide; CD, cluster of differentiation; CHB, chronic hepatitis B; CTLs, cytotoxic T lymphocytes; DC, dendritic cell; FasL, Fas ligand; FHB, fulminant hepatitis B; HBcAg, hepatitis B core antigen; HBsAg, hepatitis B surface antigen; HBV, hepatitis B virus; HLA, human leukocyte antigen; HSA, human serum albumin; IFN, interferon; IP, intraperitoneally; ISG, interferon-stimulated gene; mAb, monoclonal antibody; mDC, myeloid DC; mRNA, messenger RNA; NK, natural killer; PBMCs, peripheral blood mononuclear cells; PCR, polymerase chain reaction; pDC, plasmacytoid DC; SCID, severe combined immunodeficiency; TUNEL, terminal deoxynucleotidyl transferase dUTP nick end labeling; uPA, urokinase-type plasminogen activator.

From the [1]Department of Medicine and Molecular Science, Division of Frontier Medical Science, Programs for Biomedical Research, Graduate School of Biomedical Sciences, Hiroshima University, Hiroshima, Japan; [2]Liver Research Project Center, Hiroshima University, Hiroshima, Japan; [3]Laboratory for Digestive Diseases, Center for Genomic Medicine, RIKEN, Hiroshima, Japan; [4]PhoenixBio Co., Ltd., Higashi-Hiroshima, Japan; and [5]Department of Surgery, Division of Frontier Medical Science, Programs for Biomedical Research, Graduate School of Biomedical Science, Hiroshima University, Hiroshima, Japan.

Received August 16, 2011; accepted February 4, 2012.

This study was supported, in part, by a Grant-in-Aid for Scientific Research from the Japanese Ministry of Labor, Health, and Welfare.

development of fulminant hepatitis.[7,8] CTLs can kill target cells using two distinct lytic pathways: the degranulation pathway, in which perforin is used to puncture the membranes of infected cells, and the Fas-based pathway, in which the interaction between Fas ligand (FasL) expressed on cytolytic lymphocytes and Fas on target cells triggers apoptosis and target cell death.[9] However, the role of innate immune cells, especially natural killer (NK) cells, in fulminant hepatitis remains obscure. NK cells have recently been reported to contribute to the pathogenesis of human hepatitis and animal models of liver injury.[10,11] Replication of HBV is host cell dependent, and the study of cellular immune response in hepatitis B has long been hampered by the lack of a small animal model that supports the replication of HBV and elimination of infected cells by immune response. Before the advent of human hepatocyte chimeric mice,[12,13] only chimpanzees had been used as a model for HBV infection and inflammation, although fulminant hepatitis B (FHB) had never been reported, and severe liver inflammation is rare in chimpanzees.[14] We previously established an HBV-infection animal model using chimeric mice, in which the livers were extensively repopulated with human hepatocytes.[15-17] In this study, we attempted to establish an animal model of HBV-infected human hepatocytes with human immunity by transplanting human peripheral mononuclear cells (PBMCs) to HBV-infected human hepatocyte chimeric mice.

Materials and Methods

Generation of Human Hepatocyte Chimeric Mice. Generation of the urokinase-type plasminogen activator (uPA)$^{+/+}$/severe combined immunodeficiency (SCID)$^{+/+}$ mice and transplantation of human hepatocytes with human leukocyte antigen (HLA)-A0201 were performed as described previously.[15,16] All mice were transplanted with frozen human hepatocytes obtained from the same donor. Infection, extraction of serum samples, and euthanasia were performed under ether anesthesia. Concentration of human albumin, which is correlated with the repopulation index,[15] was measured in mice as described previously.[16] All animal protocols described in this study were performed in accord with the *Guide for the Care and Use of Laboratory Animals* and the local committee for animal experiments, and the experimental protocol was approved by the Ethics Review Committee for Animal Experimentation of the Graduate School of Biomedical Sciences at Hiroshima University (Hiroshima, Japan).

Human Serum Samples. Human serum samples, containing high titers of genotype C HBV DNA (5.3×10^6 copies/mL), were obtained from patients with chronic hepatitis who provided written informed consent. Individual serum samples were divided into aliquots and stored in liquid nitrogen. Six weeks after hepatocyte transplantation, chimeric mice were injected intravenously with 50 μL of HBV-positive human serum.

Analysis of HBV. DNA was extracted using SMITEST (Genome Science Laboratories, Tokyo, Japan) and dissolved in 20 μL of H_2O. HBV DNA was measured by real-time polymerase chain reaction (PCR) using a light cycler (Roche, Mannheim, Germany). Primers used for amplification were 5′-TTTGGGCATGGACATTGAC-3′ and 5′-GGTGA ACAATGTTCCGGAGAC-3′. Amplification conditions included initial denaturation at 95°C for 10 minutes, followed by 45 cycles of denaturation at 95°C for 15 seconds, annealing at 58°C for 5 seconds, and extension at 72°C for 6 seconds. The lower detection limit of this assay was 300 copies.

Preparation of Human Blood Mononuclear Cells and Transplantation of Human PBMCs Into Human Hepatocyte Chimeric Mice. PBMCs were isolated from healthy blood donors with HLA-A0201 and successfully vaccinated with recombinant yeast-derived hepatitis B surface antigen (HBsAg) vaccine (Bimmugen; Chemo-Sero Therapeutic Institute, Kumamoto, Japan) using Ficoll-Hypaque density gradient centrifugation. Neither monocytes nor macrophages were observed in the isolated PBMCs (Supporting Fig. 1). PBMCs isolated from 3 healthy, unvaccinated blood donors were also transplanted. Eight weeks after HBV inoculation, human PBMCs were transplanted into human hepatocyte chimeric mice. To deplete mouse NK cells and prevent the elimination of human PBMCs from human hepatocyte

Address reprint requests to: Kazuaki Chayama, M.D., Ph.D., Department of Medical and Molecular Science, Division of Frontier Medical Science, Programs for Biomedical Research, Graduate School of Biomedical Science, Hiroshima University, 1-2-3 Kasumi, Minami-ku, Hiroshima 734-8551, Japan. E-mail: chayama@hiroshima-u.ac.jp; fax: +81-82-255-6220.

View this article online at wileyonlinelibrary.com.
DOI 10.1002/hep.25651
Potential conflict of interest: The authors have no conflicts to disclose.
Additional Supporting Information may be found in the online version of this article.

chimeric mice, 200 μL of phosphate-buffered saline, containing 120 μL of anti–ganglio-N-tetraosylceramide (asialo GM1) antibody (Wako, Osaka, Japan), were administered intraperitoneally (IP) 1 day before (day 0; Fig. 1) the initial IP transplantation (day 1) of human PBMC. Then, 10 μL/g of liposome-encapsulated clodronate (Sigma-Aldrich, St. Louis, MO) were also administered 4 days before PBMC transplantation (day −2) to deplete mouse macrophages and DC cells. The second PBMC administration (4×10^7 cells/mouse) was performed 2 days after the initial administration (day 3).

To assess the effect of the depletion of human DC, NK, or CD8-positive CTL cells from administered PBMCs on hepatitis formation, the BD IMag separation system (BD Biosciences, Franklin Lakes, NJ) was used. Alternatively, mice were treated with an IP administration of clodronate, as described above, 1 day before PBMC transplantation.

To analyze the effect of inhibition of the Fas/FasL system, IFN-γ, IFN-α, antihuman FasL monoclonal antibody (mAb) (1.5 mg/mouse; R&D Systems, Minneapolis, MN), antihuman IFN-γ mAb (1.5 mg/mouse; R&D Systems), and antihuman IFN-α mAb (1.5 mg/mouse; PBL Biomedical Laboratories, Piscataway, NJ) were injected 1 day before transplantation of human PBMCs.

Flow Cytometry. Reconstructed human PBMC proliferation in mice was determined by flow cytometry with the following mAbs used for PBMC surface staining: allophycocyanin (APC)-H7 antihuman CD3 (clone SK7); APC-conjugated anti-CD4 (clone SK); BD Horizon V450 antihuman CD8 (clone RPA-T8); APC-conjugated antihuman CD11c (clone B-ly6); HU HRZN V500 MAB-conjugated antihuman CD45 (clone H130); Alexa Fluor 488–conjugated antihuman CD56 (clone B159); PerCP-Cy5.5 antihuman CD123 (clone 7G3); fluorescein isothiocyanate–conjugated Lineage cocktail 1 (Lin-1) (anti-CD3, CD14, CD16, CD19, CD20, and CD56); APC-H7 antihuman HLA-DR (clone L243); phycoerythrin (PE)-conjugated antihuman FasL (clone NOK-1); and biotin-conjugated antimouse H-2D^b (clone KH95). The biotinylated mAbs were visualized using PE-Cy7-streptavidin. Each of the above mAbs were purchased from BD Biosciences. PE-conjugated HBV core-derived immunodominant CTL epitope (HBcAg93)[18] (Medical & Biological Laboratories Co., Ltd., Nagoya, Japan). Dead cells identified by light scatter and propidium iodide staining were excluded from the analysis. Flow cytometry was performed using a FACSAria II flow cytometer (BD Biosciences), and results were analyzed with FlowJo software (Tree Star, Inc., Ashland, OR).

DCs can be classified into two main subsets: plasmacytoid DCs (pDCs) and myeloid DCs (mDCs).[19,20] pDCs were defined as CD45$^+$Lin-1$^-$HLA-DR$^+$CD123$^+$ cells, whereas mDCs were defined as CD45$^+$ Lin-1$^-$HLA-DR$^+$CD11c$^+$ cells.

Histochemical Analysis of Mouse Liver and Terminal Deoxynucleotidyl Transferase dUTP Nick End Labeling Assay. Histochemical analysis and immunohistochemical staining using an antibody against human serum albumin (HSA; Bethyl Laboratories, Inc., Montgomery, TX), an antibody against hepatitis B core antigen (HBcAg) (Dako Diagnostika, Hamburg, Germany) and antibody against Fas (BD Biosciences, Tokyo, Japan) were performed as described previously.[16] Immunoreactive materials were visualized using a streptavidin-biotin staining kit (Histofine SAB-PO kit; Nichirei, Tokyo, Japan) and diainobenzidine. For the terminal deoxynucleotidyl transferase dUTP nick end labeling (TUNEL) assay in sliced tissues, we used an *in situ* cell death detection kit (POD; Roche Diagnostics Japan, Tokyo, Japan).

Dissection of Mouse Livers and Isolation of RNA and Measurement of Messenger RNAs of Fas by Reverse-Transcription PCR. Mice were sacrificed by anesthesia with diethyl ether, and livers were excised, dissected into small sections, and then snap-frozen in liquid nitrogen. Total RNA was extracted from cell lines using the RNeasy Mini Kit (Qiagen, Valencia, CA). One microgram of each RNA sample was reverse transcribed with ReverseTra Ace (Toyobo Co., Tokyo, Japan) and Random Primer (Takara Bio Inc., Kyoto, Japan). We analyzed the messenger RNA (mRNA) levels of Fas by reverse-transcription PCR, as previously reported, using Fas forward primer 5′-GGGCATCTGGACCCTCCTA-3′ and Fas reverse primer 5′- GGCATTAACACTTTTGGACGATAA-3′.

Statistical Analysis. mRNA expression levels of Fas and interferon-stimulated genes (ISGs) were compared using Mann-Whitney's U test and unpaired *t* tests. A *P* value less than 0.05 was considered statistically significant.

Results

Establishment of an Animal Model of Fulminant Hepatitis Using HBV-Infected Human Hepatocyte Chimeric Mice and Human PBMC Transplantation. Administration of 2×10^7 PBMCs twice after suppression of mice NK cells by anti–asialo GM1 antibody[21] and macrophages and DCs by liposome-encapsulated clodronate[22] before transplantation

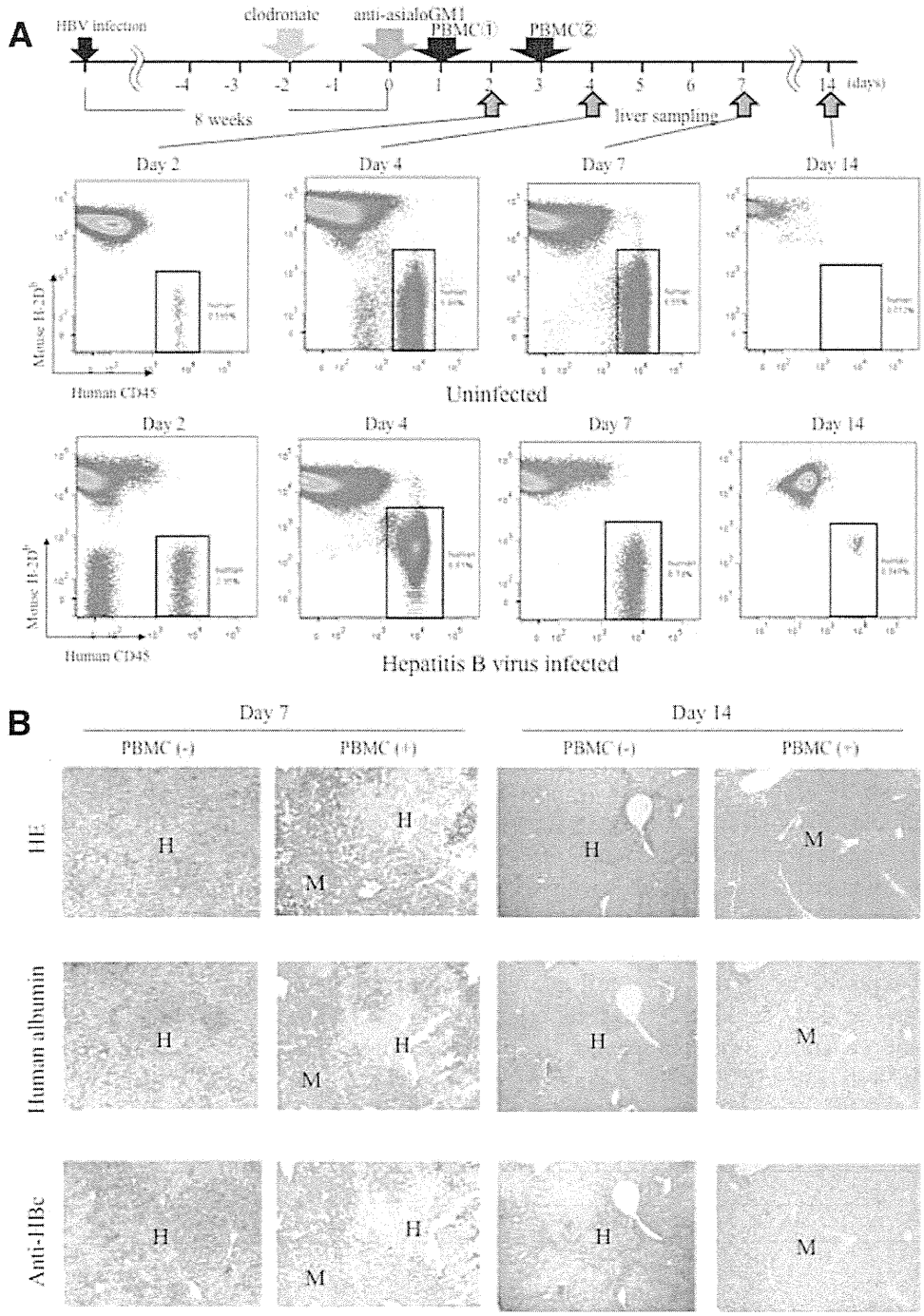

Fig. 1. Establishment of human PBMC chimerism in human hepatocyte chimeric mice. (A) Experimental protocol to establish chimerism and liver sampling is shown at the top of the figure (see Materials and Methods). Scheduling of administration of HBV-positive serum, clodronate, and anti-asialo GM1 antibody and liver sampling by scarification are shown by arrows. Liver mononuclear cells isolated from uninfected (upper panel) and HBV-infected (lower panel) human hepatocyte chimeric mice transplanted with human PBMCs were separated with antibodies for human CD45 and mouse H-2D^b and were analyzed by flow cytometry. Percentage of human mononuclear cells is shown in each panel. Representative figures of two experiments with similar results are shown. (B) Histological analysis of livers of HBV-infected mice. Liver samples obtained from mice with or without human PBMCs at weeks 9 (day 7) and 10 (day 14) were stained with hematoxylin and eosin staining (HE), anti-human albumin antibody, or anti-hepatitis B core antibody. Regions are shown as human (H) and mouse (M) hepatocytes, respectively (original magnification, 40×). (C) Time course of human albumin concentration (upper panel) and HBV DNA titer (lower panel) in mouse serum. Time course of 4 HBV-infected mice transplanted with human PBMCs, 3 HBV-infected mice without human PBMC transplantation, and 4 uninfected mice transplanted with human PBMC are shown. (D) Time course of human albumin concentration (upper panel) and HBV DNA titer (lower panel) in mice. Mice with or without HBV-infection were transplanted with PBMCs obtained from 3 healthy donors who were not vaccinated against hepatitis B.

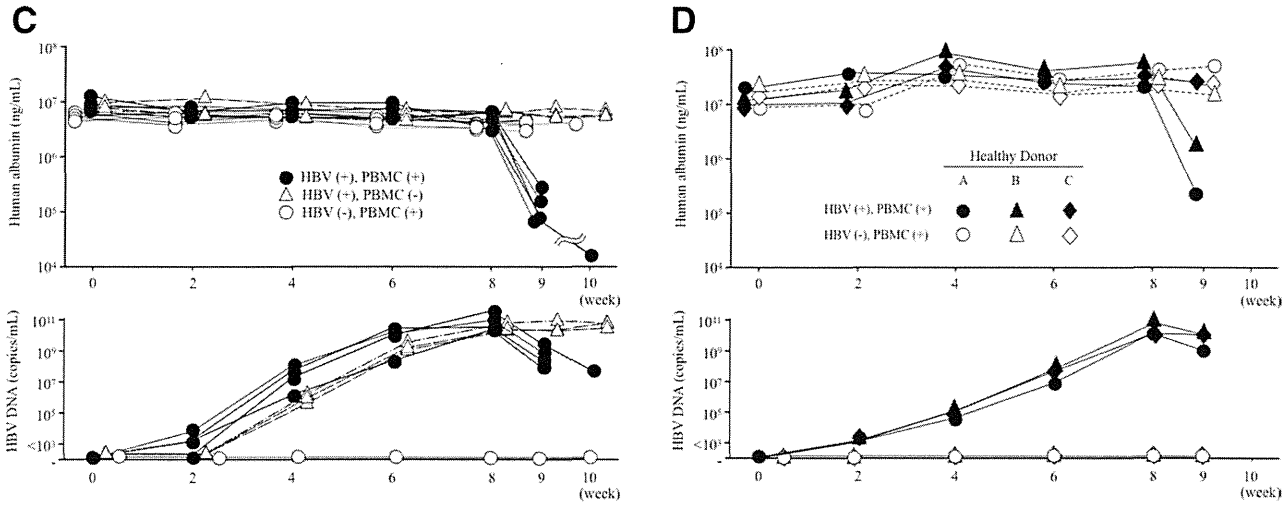

Fig. 1.

enabled us to establish a human PBMC chimerism in uPA-SCID mice. We observed an up to 7% human mononuclear cell chimerism among the liver-resident mononuclear cells of uninfected and HBV-infected mice 2-14 days after the initial injection of PBMC (Fig. 1A; Table 1). Chimerism was most prominent 4 days after initial PBMC administration and almost undetectable by day 14 (Fig. 1A). Histological examination of chimeric mice livers showed extensive human liver cell death, comparable to the massive liver cell death observed in fulminant hepatitis, only in HBV-infected and PBMC-treated mice liver (Fig. 1B). Human hepatocytes were almost completely eliminated and replaced by human albumin-negative mouse hepatocytes at days 7 and 14. Consistent with these histological changes, we observed a rapid decline of HSA levels and HBV DNA only in HBV-infected and PBMC-treated mice (Fig. 1C). The decline of mice HSA levels and HBV DNA was also observed in 2 of 3 HBV-infected mice transplanted with PBMCs isolated from healthy blood donors without HBsAg vaccination (Fig. 1D and Supporting Fig. 2).

Analysis of Liver-Infiltrating Human Lymphocytes Necessary to Establish Massive Hepatocyte Degeneration. We then analyzed liver-infiltrating cells with flow cytometry. Unexpectedly, we did not detect CD8-positive and tetramer-positive CTLs, as reported previously (Fig. 2A). Instead, we observed substantial numbers of CD3-negative and CD56-positive NK cells (Fig. 2B) and small numbers of pDCs and mDCs (Fig. 2C). The majority of NK cells of HBV-infected mice were FasL positive (Fig. 2D). In contrast, such FasL-positive NK cells were not detected in uninfected

Table 1. Analysis of Liver-Infiltrating Cells by Flow Cytometry

	HBV Infected				Uninfected			
Day	No.	Chimerism (%)	Human NK (%)	Fas (+) NK (%)	No.	Chimerism (%)	Human NK (%)	FasL (+) NK (%)
2	1	1.77	2.51	0	1	0.59	12.8	0
	2	2.35	3.02	0.143	2	0.774	58.8	1.1
4	3	6.81	30.7	80.1	3	5.95	42.7	0.678
	4	1.08	68.7	94.7	4	7.11	4.98	0.027
	5	6.60	23.2	58.7	5	5.02	23.1	0.314
7	6	6.73	13.2	0.383	6	6.55	42.1	0.103
	7	5.70	12.5	2.01	7	1.24	13.6	0.025
	8	1.46	3.83	0	8	2.04	1.49	4.03
14	9	0.34	ND	ND	9	0.012	ND	ND
	10	NA*	NA	NA	10	0.013	ND	ND
DCs depleted day 4	11	4.77	5	2.14	11	3.32	4.21	0.465
(by clodronate)	12	1.27	39.5	2.3	12	12.9	9.06	0
DCs depleted day 7	13	2.42	24.8	2.19	13	6.31	54.1	0.131
(by clodronate)	14	1.41	10.6	0.103	14	4.69	1.68	0.12

Abbreviations: NA, not analyzed; ND, not detectable.
*Mouse died just before liver analysis.

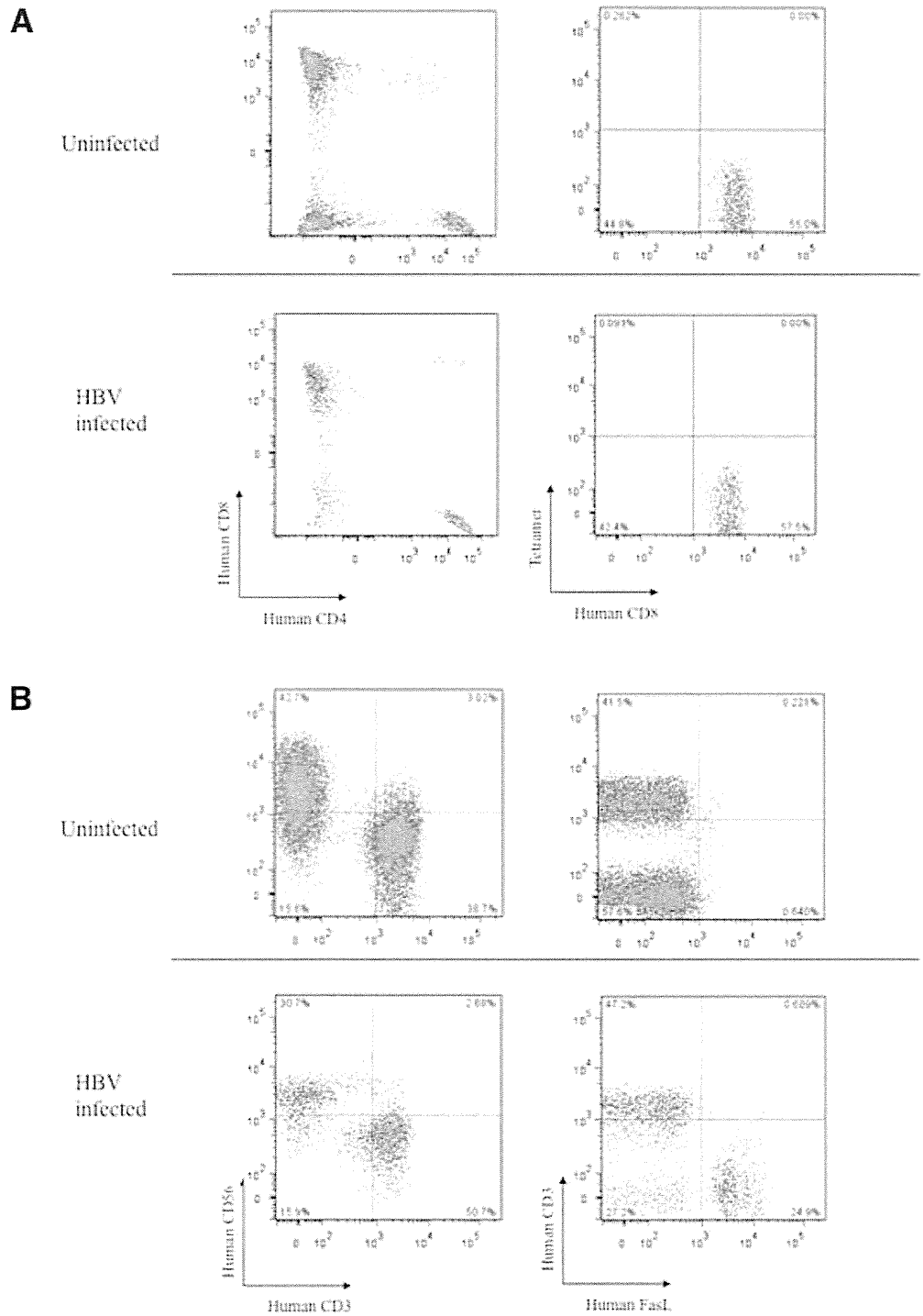

Fig. 2. Analysis of mononuclear cells isolated from day 4 chimeric mouse livers. After defining human PBMCs as mouse H-2Db-human CD45^{+} cells, we further analyzed the phenotypes of these cells. (A-C) Liver mononuclear cells of uninfected (upper panel) and HBV-infected (lower panel) mice transplanted with human PBMCs were separated with anti-human CD4 and CD8 antibody or anti-human CD8 and HLA-A2 HBcAg tetramer (A), anti-human CD3and CD56 or human CD3 and FasL (B), and anti-human HLA-DR and CD123 and HLA-DR and CD11c (C). (D) Frequency of FasL-positive cells in NK cells were analyzed in uninfected and HBV-infected mice. All figures are representative of two experiments with similar results.

mice livers (Table 1; Fig. 2D), suggesting that these NK cells were activated in HBV-infected mice. These activated NK cells and DCs were detectable in mice livers only 4 days after the initial PBMC injection, but were undetectable after 2 and 7 days (Supporting Figs. 3 and 4, respectively).

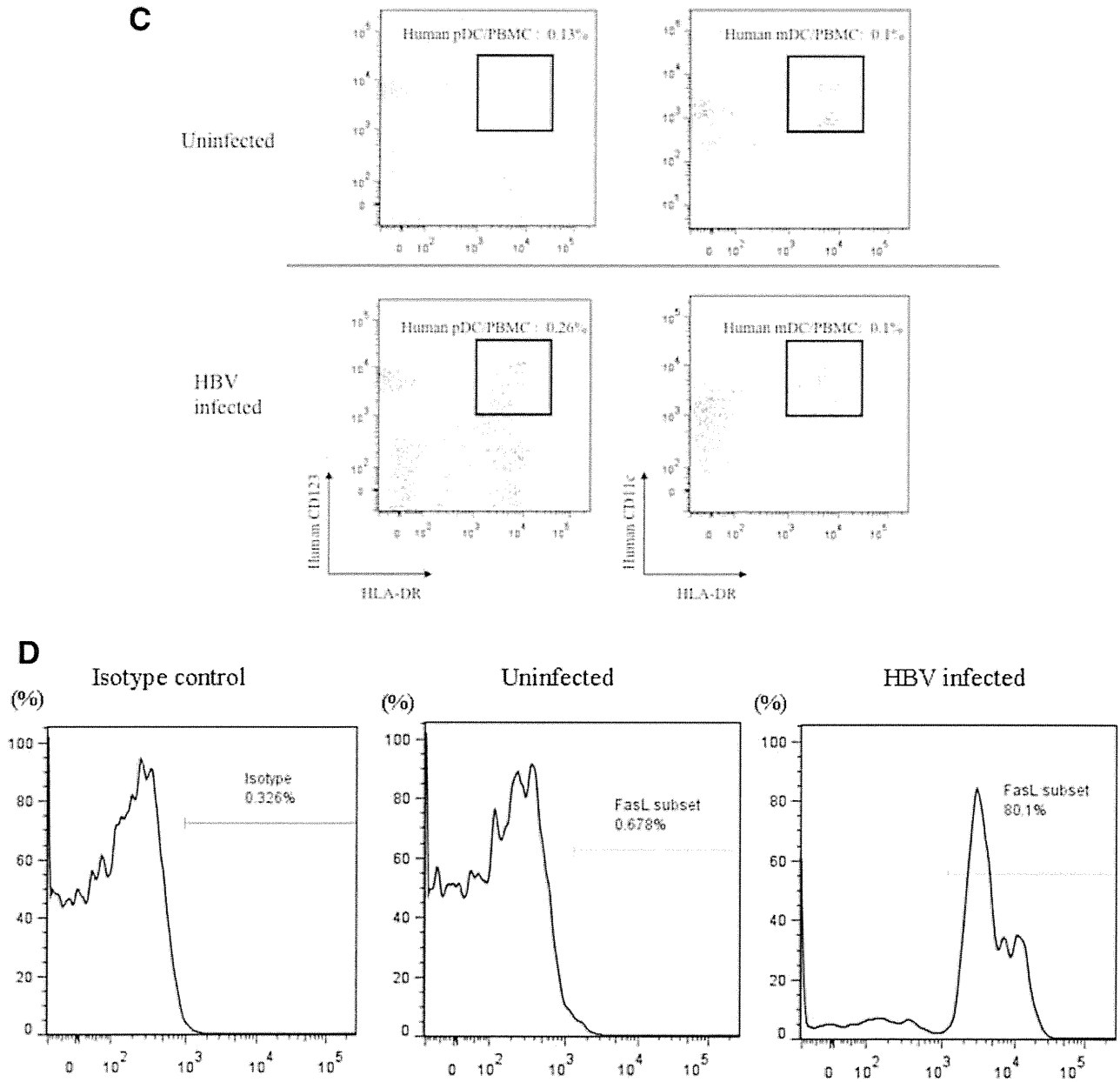

Fig. 2.

Effect of DC Depletion on Establishment of Massive Hepatocyte Degeneration. To confirm the necessity of both DCs and NK cells to complete hepatocyte destruction, we depleted DCs or NK cells with negative selection using antibody-coated magnetic beads before the administration of PBMC. Depletion of either DCs or NK cells completely abolished the decline of human albumin as well as HBV DNA (Supporting Fig. 5A). However, analysis of liver-infiltrating cells revealed that chimerism with human PBMC was poorly established in these animals, probably the result of the loss or damage of human cells by bound antibodies during separation and/or subsequent incubation in mice (Supporting Fig. 5B; Supporting Table 1).

To overcome possible confounding resulting from poor chimerism resulting in poor human hepatocyte degeneration in mice, we attempted to remove DCs from transplanted human PBMCs by alternate means. We attempted to deplete human DCs by administering clodronate 1 day before PBMC transplantation, because we thought that clodronate remaining in the mouse body would impair transplanted human DCs. As expected, we observed an almost complete elimination of DCs by this procedure without impairing

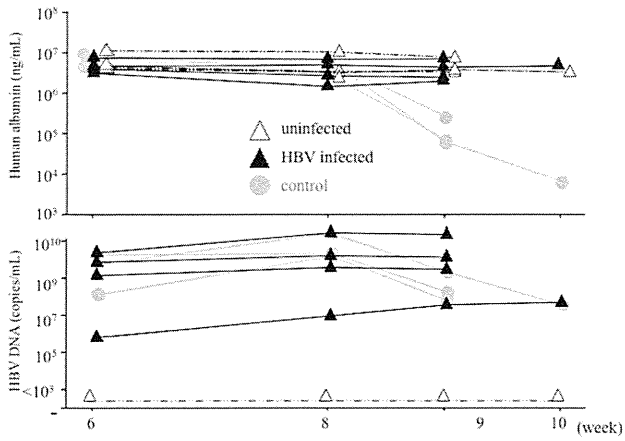

Fig. 3. Time course of mice transplanted with human PBMCs with DC depletion by clodronate 1 day before transplantation. Mice were treated with IP administration of clodronate 1 day before human PBMC transplantation. Time courses of human albumin concentration (upper panel) and HBV DNA titer (lower panel) in mouse serum are shown. Open and closed triangles correspond to 3 uninfected and 4 HBV-infected mice, respectively. Time courses of 3 mice infected with HBV and transplanted with human PBMC 3 days before transplantation (see Fig. 1C) are shown for comparison (shaded closed circle).

PBMC chimerism (Supporting Figs. 6A and 7A; Supporting Table 1). Activation of NK cells was not observed in this setting (Supporting Figs. 6B and 7B; Supporting Table 1). Depletion of DCs completely abolished the decline of both human albumin and HBV DNA (Fig. 3). Histological examination showed that hepatocyte degeneration was absent, and that there were no TUNEL-staining–positive cells (data not shown). Clodronate lyposomes may also nonspecifically deplete macrophages and monocytes in addition to DCs, but no monocytes or macrophages were observed when transplanted PBMCs were analyzed using Ficoll-Hypaque density gradient centrifugation, indicating that the clodronate administration was specifically associated with DC depletion in this study.

Analysis of Fas/FasL System in Massive HBV-Infected Hepatocyte Degeneration Model. We then assessed the importance of the Fas/FasL system and the occurrence of apoptosis in NK-cell–mediated human hepatocyte degeneration. Only HBV-infected human hepatocytes positive for HSA were positive for Fas antibody staining (Fig. 4A). TUNEL staining was also positive only in mice infected with HBV and inoculated with PBMCs (days 4 and 7). Measurement of mRNA levels in infected and uninfected livers showed that expression levels of Fas mRNA increased significantly upon HBV infection (Fig. 4B). To confirm that apoptosis of human hepatocytes was mediated by the Fas/FasL pathway and to determine whether IFN-α or IFN-γ played a role in the establishment of liver cell degeneration, we administered a blocking mAb against FasL, IFN-α, and IFN-γ 1 day before PBMC transplantation. Treatment of mice with antibody against FasL before PBMC completely abolished the decline of human albumin and HBV DNA (Fig. 5A). This abolishment of human albumin decline in mouse serum suggests that the Fas/FasL pathway almost exclusively eliminated infected hepatocytes in this model, which also suggests that Fas-mediated apoptosis could play an important role in FHB. Antibodies against IFN-α and IFN-γ inhibited IFN-induced ISG expression in mice livers (Supporting Fig. 8); however, these antibodies did not disturb the decline of HSA levels (Fig. 5A) and histological inflammation (Fig. 5B). Contact-dependent and -independent activation of NK cells by DCs has been reported previously.[23-25] Although IFN-α and IFN-γ play a role in their activation,[23,25,26] our results indicate that the effects of IFN-α are almost negligible in our experiments (Fig. 5A), suggesting that direct contact among these cells, or cytokines other than IFN-α and IFN-γ, are necessary to activate NK cells in this setting. NK cells have also been reported to exert antiviral effects by secreting IFN-γ. However, our results suggest that this mechanism does not work well in our model (Fig. 5A).

Discussion

In this study, we established a small animal model in which massive hepatocyte degeneration similar to FHB in humans is observed. Our initial attempts to detect human PBMCs in blood or any organ in transplanted mice failed even after injecting 2×10^7 cells, which is sufficient to establish human PBMC chimerism in SCID mice.[27] We assumed that failure to develop chimerism was the result of the activity of NK cells and macrophages because the activity of these cells in uPA-SCID mice is higher than in SCID mice.[28,29] Therefore, we attempted to eliminate these effects by administering clodronate and anti–asialo GM1 antibody, which are known to effectively eliminate these cells.[30,31] This assumption appears to be valid, because we were able to establish human PBMC chimerism and massive hepatocyte degeneration by suppressing these cells (Fig. 1).

HBV-specific CTLs have been reported to play an important role in eliminating the virus.[32-34] Accordingly, we attempted to detect HBV-specific CTLs in mice with massive hepatocyte degeneration. Unexpectedly, we failed to detect HBV-specific CTLs (Fig. 2A and Supporting Fig. 9) and instead found that infiltrating cells in the liver were CD3-negative NK cells

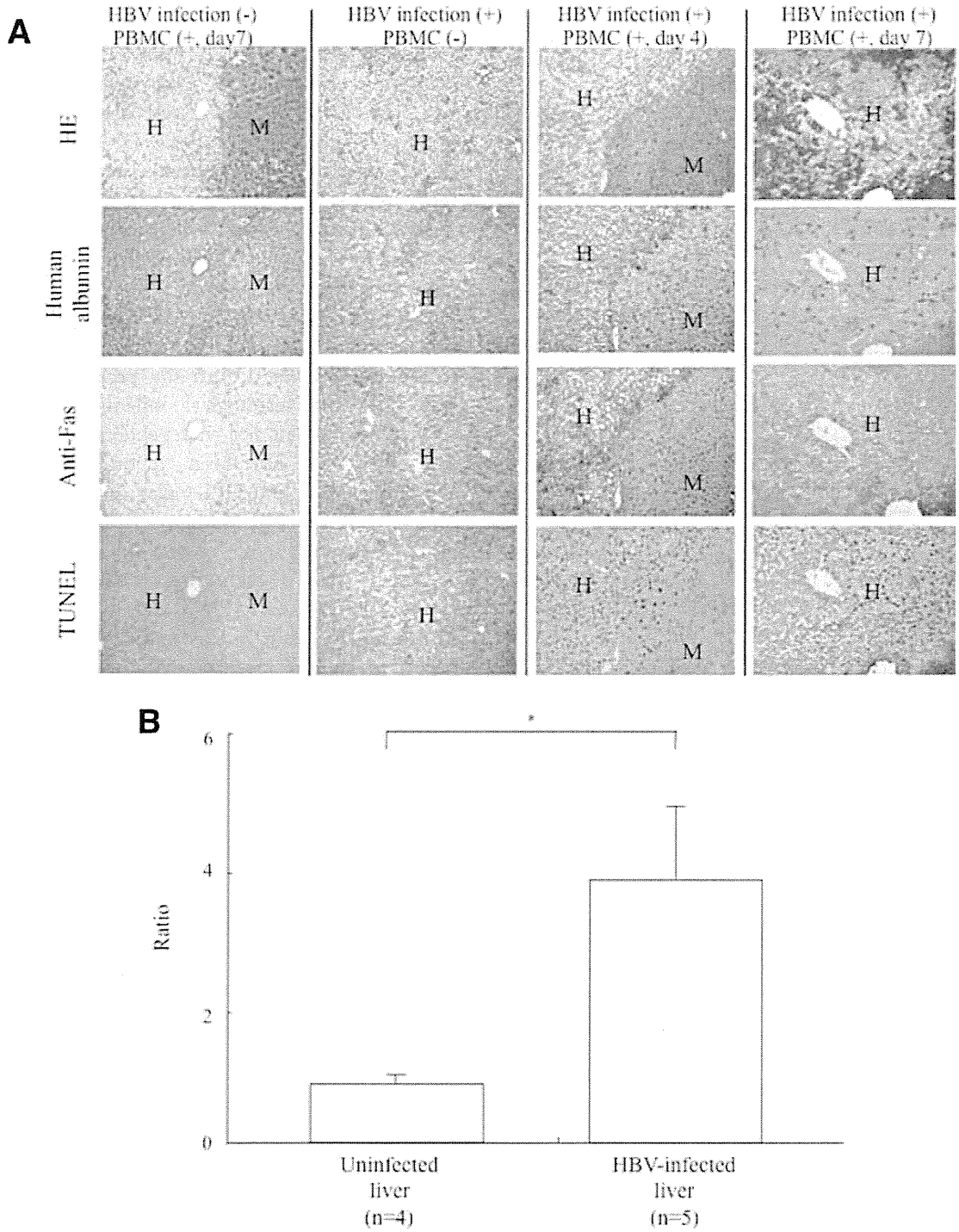

Fig. 4. Assessment of Fas expression in the liver in human hepatocyte chimeric mice. (A) Histological analysis of chimeric mice livers transplanted with human PBMCs but without HBV infection (day 7), with HBV infection but without PBMC transplantation, and with HBV infection and PBMC transplantation at days 4 and 7. Liver samples were stained with hematoxylin and eosin staining (HE), anti-human albumin antibody, anti-human Fas antibody, and TUNEL staining. Regions are shown as human (H) and mouse (M) hepatocytes, respectively (original magnification, 100×). Note that Fas antigen was expressed only in HBV-infected human hepatocytes, and TUNEL staining is only positive for HBV-infected and human PBMC-transplanted mice livers. Mouse hepatocytes were negative for all three stains. (B) Expression of Fas mRNA levels in uninfected and HBV-infected human hepatocytes. Data are represented as mean ± standard deviation. *$P < 0.001$.

(Fig. 2B,D and Supporting Fig. 10). The reason for the absence of CTLs in our experiment is unknown, but this suggests that massive hepatocyte degeneration resembling fulminant hepatitis can be caused by NK cells as a main player, and recent reports demonstrating that NK cells contribute to severe acute and

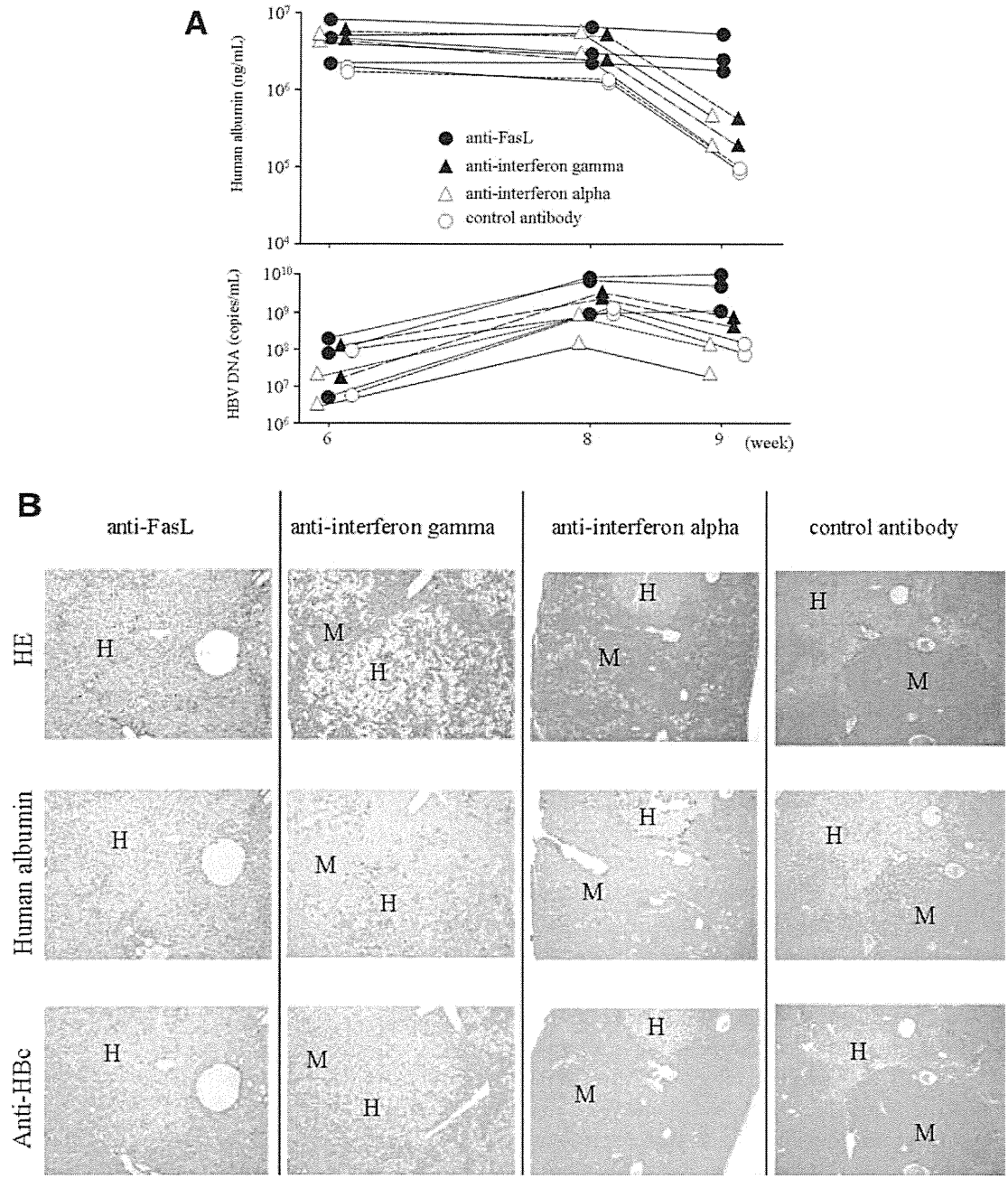

Fig. 5. Effect of anti-FasL, anti-IFN-γ and anti-IFN-α antibody administration on HSA and HBV DNA. (A) Time courses of HSA (upper panel) and HBV DNA (lower panel) before and 1 week after human PBMC transplantation are shown. Mice were pretreated with antibodies against human Fas-L, IFN-γ, and IFN-α before PBMC transplantation, as described in Materials and Methods. Isotype antibody was used as a control. (B) Histological analysis of livers of HBV-infected mice injected with anti-human FasL mAb, IFN-γ, IFN-α, and control antibody. Liver samples obtained from mice with human PBMCs at weeks 9 (day 7) were stained with hematoxylin and eosin staining (HE), antihuman albumin antibody, or antihepatitis B core antibody. Regions are shown as human (H) and mouse (M) hepatocytes, respectively (original magnification, 40×).

chronic hepatitis B (CHB) support this assertion.[11,35] We attempted to collect CTLs from HBV-infected patients and to establish hepatitis in chimeric mice. However, we rarely detected tetramer-positive CTLs in blood samples from chronically infected patients and were therefore unable to establish hepatitis using CD8-positive T cells. Consequently, a limitation of this study is that differential roles of NK cells and CTLs in massive liver cell death could not be examined.

Although it is not clear in this study how profoundly DC and NK cell activity plays a role in patients with FHB, our results suggest that the immune system can trigger severe hepatocyte

degeneration. The importance of the activation of NK cells by DCs was evident, because depletion of DCs almost completely abolished the massive hepatocyte degeneration in this model (Supporting Fig. 10; Table 1). The interaction between NK cells and DCs is not well characterized, although it has been established that antigen-presenting accessory cells provide both indirect (i.e., soluble) and direct (i.e., contact-dependent) signals to T cells. Experiments in which NK cells are separated from pathogens and antigen-presenting cells by semipermeable membranes are cultured with supernatants from pathogen-activated DCs or in which cytokines are neutralized with blocking antibodies. These reports indicate that both soluble and contact-dependent signals may contribute to the activation of NK cells.[23,25,26]

The importance of the Fas/FasL system in hepatocyte damage in acute and chronic HBV infection has been reported previously.[37,38] However, the extent to which this system plays a role in human hepatitis B, especially fulminant hepatitis, is unknown. As shown in this study (Fig. 5A), inhibition of the Fas/FasL system by anti-Fas antibody dramatically reduced the effect of human PBMC transplantation. This showed the possibility that the Fas/FasL system plays an important role in the degeneration of infected hepatocytes in FHB. Further studies should be conducted to evaluate what immunological responses play important roles in human hepatitis B.

The importance of NK-cell activity suggests that the suppression of DCs and NK-cell activity or the Fas/FasL system might have therapeutic implications for FHB.[11,35] If DCs and NK-cell activity or Fas/FasL activity could be controlled in the early stages of severe acute or fulminant hepatitis, we might be able to control hepatitis activity and prevent subsequent liver failure. Of course, it would be necessary to monitor the development of chronic hepatitis after such treatment because DCs and NK cells contribute to early host defenses and shape subsequent adaptive immune response through complex cross-talk regulating the early phase of the immune response.[19,24,39,40]

We analyzed liver damage using HBV genotype C–infected mice in this study. However, HBV genotype C is associated with more severe histological liver damage than genotype B,[41] and future studies should compare immunological differences between genotypes B and C.

In summary, we established an animal model of FHB using highly repopulated human hepatocyte chimeric mice and transplanted human PBMCs. Modifications of this model will facilitate further research into acute and CHB using human immune cells, including HBV-directed CTL clones, suppressor and regulatory T cells, as well as immunological experiments to study interactions between DCs and NK cells. Such models may be useful to develop and evaluate new therapeutic strategies against HBV infection.

Acknowledgment: The authors thank Rie Akiyama and Yoko Matsumoto for their expert technical assistance. This work was carried out at the Analysis Center of Life Science, Natural Science Center for Basic Research and Development, Hiroshima University.

References

1. Bernal W, Auzinger G, Dhawan A, Wendon J. Acute liver failure. Lancet 2010;376:190-201.
2. Leifeld L, Cheng S, Ramakers J, Dumoulin FL, Trautwein C, Sauerbruch T, Spengler U. Imbalanced intrahepatic expression of interleukin 12, interferon gamma, and interleukin 10 in fulminant hepatitis B. HEPATOLOGY 2002;36:1001-1008.
3. Ozasa A, Tanaka Y, Orito E, Sugiyama M, Kang JH, Hige S, et al. Influence of genotypes and precore mutations on fulminant or chronic outcome of acute hepatitis B virus infection. HEPATOLOGY 2006;44:326-334.
4. Kawai T, Akira S. Toll-like receptor and RIG-I-like receptor signaling. Ann N Y Acad Sci 2008;1143:1-20.
5. Maini MK, Boni C, Lee CK, Larrubia JR, Reignat S, Ogg GS, et al. The role of virus-specific CD8(+) cells in liver damage and viral control during persistent hepatitis B virus infection. J Exp Med 2000;191:1269-1280.
6. Guidotti LG, Ando K, Hobbs MV, Ishikawa T, Runkel L, Schreiber RD, Chisari FV. Cytotoxic T lymphocytes inhibit hepatitis B virus gene expression by a noncytolytic mechanism in transgenic mice. Proc Natl Acad Sci U S A 1994;91:3764-3768.
7. Ando K, Moriyama T, Guidotti LG, Wirth S, Schreiber RD, Schlicht HJ, et al. Mechanisms of class I restricted immunopathology. A transgenic mouse model of fulminant hepatitis. J Exp Med 1993;178:1541-1554.
8. Cote PJ, Toshkov I, Bellezza C, Ascenzi M, Roneker C, Ann Graham L, et al. Temporal pathogenesis of experimental neonatal woodchuck hepatitis virus infection: increased initial viral load and decreased severity of acute hepatitis during the development of chronic viral infection. HEPATOLOGY 2000;32:807-817.
9. Chisari FV. Rous-Whipple Award Lecture. Viruses, immunity, and cancer: lessons from hepatitis B. Am J Pathol 2000;156:1117-1132.
10. Dunn C, Brunetto M, Reynolds G, Christophides T, Kennedy PT, Lampertico P, et al. Cytokines induced during chronic hepatitis B virus infection promote a pathway for NK cell-mediated liver damage. J Exp Med 2007;204:667-680.
11. Zhang Z, Zhang S, Zou Z, Shi J, Zhao J, Fan R, et al. Hypercytolytic activity of hepatic natural killer cells correlates with liver injury in chronic hepatitis B patients. HEPATOLOGY 2011;53:73-85.
12. Dandri M, Burda MR, Torok E, Pollok JM, Iwanska A, Sommer G, et al. Repopulation of mouse liver with human hepatocytes and *in vivo* infection with hepatitis B virus. HEPATOLOGY 2001;33:981-988.
13. Petersen J, Burda MR, Dandri M, Rogler CE. Transplantation of human hepatocytes in immunodeficient UPA mice: a model for the study of hepatitis B virus. Methods Mol Med 2004;96:253-260.
14. Ogata N, Miller RH, Ishak KG, Purcell RH. The complete nucleotide sequence of a pre-core mutant of hepatitis B virus implicated in fulminant hepatitis and its biological characterization in chimpanzees. Virology 1993;194:263-276.

15. Tateno C, Yoshizane Y, Saito N, Kataoka M, Utoh R, Yamasaki C, et al. Near completely humanized liver in mice shows human-type metabolic responses to drugs. Am J Pathol 2004;165:901-912.
16. Tsuge M, Hiraga N, Takaishi H, Noguchi C, Oga H, Imamura M, et al. Infection of human hepatocyte chimeric mouse with genetically engineered hepatitis B virus. HEPATOLOGY 2005;42:1046-1054.
17. Tsuge M, Hiraga N, Akiyama R, Tanaka S, Matsushita M, Mitsui F, et al. HBx protein is indispensable for development of viraemia in human hepatocyte chimeric mice. J Gen Virol 2010;91:1854-1864.
18. Kuhober A, Pudollek HP, Reifenberg K, Chisari FV, Schlicht HJ, Reimann J, Schirmbeck R. DNA immunization induces antibody and cytotoxic T cell responses to hepatitis B core antigen in H-2b mice. J Immunol 1996;156:3687-3695.
19. Banchereau J, Steinman RM. Dendritic cells and the control of immunity. Nature 1998;392:245-252.
20. Shortman K, Liu YJ. Mouse and human dendritic cell subtypes. Nat Rev Immunol 2002;2:151-161.
21. Sandhu J, Shpitz B, Gallinger S, Hozumi N. Human primary immune response in SCID mice engrafted with human peripheral blood lymphocytes. J Immunol 1994;152:3806-3813.
22. Gonzalez SF, Lukacs-Kornek V, Kuligowski MP, Pitcher LA, Degn SE, Kim YA, et al. Capture of influenza by medullary dendritic cells via SIGN-R1 is essential for humoral immunity in draining lymph nodes. Nat Immunol 2010;11:427-434.
23. Fernandez NC, Lozier A, Flament C, Ricciardi-Castagnoli P, Bellet D, Suter M, et al. Dendritic cells directly trigger NK cell functions: cross-talk relevant in innate anti-tumor immune responses *in vivo*. Nat Med 1999;5:405-411.
24. Ferlazzo G, Tsang ML, Moretta L, Melioli G, Steinman RM, Munz C. Human dendritic cells activate resting natural killer (NK) cells and are recognized via the NKp30 receptor by activated NK cells. J Exp Med 2002;195:343-351.
25. Andoniou CE, van Dommelen SL, Voigt V, Andrews DM, Brizard G, Asselin-Paturel C, et al. Interaction between conventional dendritic cells and natural killer cells is integral to the activation of effective antiviral immunity. Nat Immunol 2005;6:1011-1019.
26. Walzer T, Dalod M, Robbins SH, Zitvogel L, Vivier E. Natural-killer cells and dendritic cells: "l'union fait la force". Blood 2005;106: 2252-2258.
27. Mosier DE, Gulizia RJ, Baird SM, Wilson DB, Spector DH, Spector SA. Human immunodeficiency virus infection of human-PBL-SCID mice. Science 1991;251:791-794.
28. Kawahara T, Douglas DN, Lewis J, Lund G, Addison W, Tyrrell DL, et al. Critical role of natural killer cells in the rejection of human hepatocytes after xenotransplantation into immunodeficient mice. Transpl Int 2010;23:934-943.
29. Morosan S, Hez-Deroubaix S, Lunel F, Renia L, Giannini C, Van Rooijen N, et al. Liver-stage development of *Plasmodium falciparum*, in a humanized mouse model. J Infect Dis 2006;193:996-1004.
30. Dorshkind K, Pollack SB, Bosma MJ, Phillips RA. Natural killer (NK) cells are present in mice with severe combined immunodeficiency (SCID). J Immunol 1985;134:3798-3801.
31. Ito M, Hiramatsu H, Kobayashi K, Suzue K, Kawahata M, Hioki K, et al. NOD/SCID/gamma(c)(null) mouse: an excellent recipient mouse model for engraftment of human cells. Blood 2002;100:3175-3182.
32. Thimme R, Wieland S, Steiger C, Ghrayeb J, Reimann KA, Purcell RH, Chisari FV. CD8(+) T cells mediate viral clearance and disease pathogenesis during acute hepatitis B virus infection. J Virol 2003;77: 68-76.
33. Rehermann B, Fowler P, Sidney J, Person J, Redeker A, Brown M, et al. The cytotoxic T lymphocyte response to multiple hepatitis B virus polymerase epitopes during and after acute viral hepatitis. J Exp Med 1995;181:1047-1058.
34. Webster GJ, Reignat S, Maini MK, Whalley SA, Ogg GS, King A, et al. Incubation phase of acute hepatitis B in man: dynamic of cellular immune mechanisms. HEPATOLOGY 2000;32:1117-1124.
35. Zou Y, Chen T, Han M, Wang H, Yan W, Song G, et al. Increased killing of liver NK cells by Fas/Fas ligand and NKG2D/NKG2D ligand contributes to hepatocyte necrosis in virus-induced liver failure. J Immunol 2010;184:466-475.
36. Newman KC, Riley EM. Whatever turns you on: accessory-cell-dependent activation of NK cells by pathogens. Nat Rev Immunol 2007; 7:279-291.
37. Galle PR, Hofmann WJ, Walczak H, Schaller H, Otto G, Stremmel W, et al. Involvement of the CD95 (APO-1/Fas) receptor and ligand in liver damage. J Exp Med 1995;182:1223-1230.
38. Rivero M, Crespo J, Fábrega E, Casafont F, Mayorga M, Gomez-Fleitas M, Pons-Romero F. Apoptosis mediated by the Fas system in the fulminant hepatitis by hepatitis B virus. J Viral Hepat 2002;9: 107-113.
39. Moretta A. Natural killer cells and dendritic cells: rendezvous in abused tissues. Nat Rev Immunol 2002;2:957-964.
40. Asselin-Paturel C, Trinchieri G. Production of type I interferons: plasmacytoid dendritic cells and beyond. J Exp Med 2005;202:461-465.
41. Orito E, Ichida T, Sakugawa H, Sata M, Horiike N, Hino K, et al. Geographic distribution of hepatitis B virus (HBV) genotype in patients with chronic HBV infection in Japan. HEPATOLOGY 2001;34: 590-594.

Microbiology and Immunology

Microbiol Immunol 2012; **56**: 318–323
doi:10.1111/j.1348-0421.2012.00439.x

ORIGINAL ARTICLE

Development of new *IL28B* genotyping method using Invader Plus assay

Satomi Kani[1,2], Yasuhito Tanaka[1,2], Kentaro Matsuura[1], Tsunamasa Watanabe[1], Hiroshi Yatsuhashi[3], Etsuro Orito[4], Ken Inose[5], Nao Motojuku[5], Yukio Wakimoto[2], and Masashi Mizokami[6]

[1]Department of Virology and Liver Unit, Nagoya City University Graduate School of Medical Sciences, [2]Department of Clinical Laboratory, Nagoya City University Hospital, [4]Nagoya Daini Red Cross Hospital, Nagoya, [3]Clinical Research Center, National Nagasaki Medical Center, Oomura, [5]Third Wave Japan Incorporated, Tokyo, [6]Research Center for Hepatitis and Immunology, National Center for Global Health and Medicine, Ichikawa, Japan

ABSTRACT

_IL28B_ polymorphism is associated with the response to pegylated interferon-α with ribavirin (PEG-IFN-α/RBV) treatment in chronic hepatitis C patients. As a genotyping assay for _IL28B_ single nucleotide polymorphisms (SNPs) in clinical practice, the Invader Plus assay was developed. The accuracy, intra-assay, inter-assay precision, and the limit of detection of the Invader Plus assay were evaluated. Two SNPs (rs8099917 and rs12979860) associated with _IL28B_ were genotyped by the Invader Plus and TaqMan assay in 512 Japanese patients. In comparison with direct sequencing, the Invader Plus assay showed 99% accuracy in rs8099917 and 100% accuracy in rs12979860. Intra-assay and inter-assay precision were sufficient to use in clinical practice and the detection limit was 1ngDNA/assay. Genotyping by rs8099917 showed that 361 (71%), 144 (28%) and seven (1%) of the patients were major homozygous, heterozygous and minor homozygous types, respectively. Five of the 512 cases (1%) had haplotype differences, but none showed differences between the two genotyping methods. For patients with HCV genotype 1, the prevalence of responders in the major homozygous type was 83.3%, and that of non-responders in the minor heterozygous/homozygous type was 72.5%. A convenient _IL28B_ genotyping method using the Invader Plus assay could be useful to predict the treatment outcome in clinical practice.

Key words interferon, *IL28B*, single nucleotide polymorphism genotyping, invader plus assay.

Hepatitis C virus (HCV) infection results in cirrhosis and hepatocellular carcinoma (HCC) worldwide (1). Pegylated interferon-α with ribavirin (PEG-IFN-α/RBV) is currently the most dominant therapy for chronic HCV infection, but roughly 50% of patients with genotype 1b, the most common in Japan, are not able to achieve a sustained virological response (SVR) determined by the serum HCV-RNA level 24 weeks after treatment (2, 3). In addition, this therapy often leads to side effects, such as flu-like symptoms, depression and anemia(4); therefore, it is valuable to predict the particular response before treatment with PEG-IFN-α/RBV to avoid these side-effects and to avoid ineffective therapy.

Not only viral factors (genotype and viral mutation), but also host factors influence the therapeutic outcome. Age, sex, body mass index and histological grade are considered to determine the individual's treatment regimen and outcome (5, 6, 7). Recently, it has been reported through a genome-wide association study (GWAS) of patients with genotype 1 HCV that single nucleotide polymorphisms (SNPs) located near the *IL28B* gene are strongly associated with a response to PEG-IFN-α/RBV

Correspondence
Yasuhito Tanaka, Department of Virology & Liver unit, Nagoya City University Graduate School of Medical Sciences, Kawasumi, Mizuho, Nagoya 467-8601, Japan.
Tel: +81 52 853 8191; fax: +81 52 842 0021; email: ytanaka@med.nagoya-cu.ac.jp

Received 19 January 2012; revised 29 January 2012; accepted 1 February 2012.

List of Abbreviations: GWAS, genome-wide association study; HCV, hepatitis C virus; NPV, negative predictive value; NVR, null virological response; PEG-IFN-α, pegylated interferon α; PPV, positive predictive value; RBV, ribavirin; SVR, sustained virological response; TVR, transient virological response.

Table 1. Primers and allele probes used for Invader Plus genotyping of *IL28B* single nucleotide polymorphisms (SNPs)

SNP		(5'-3')
rs8099917	Forward primer	TCA TCC CTC ATC CCA CTT CTG GAA CA
	Reverse primer	CGG GCC ATC TGT TTC CTG CTG
	Major allele probe	agg cca cgg acg AAT TGC TCA CAG AAA GGA A
	Minor allele probe	cgc gcc gag gCA TTG CTC ACA GAA AGG A
	Invader oligo	GCT ACC AAA CTG TAT ACA GCA TGG TTC CAA TTT GGG TGA t
rs12979860	Forward primer	GGA TGG GTA CTG GCA GCG C
	Reverse primer	AGG CGC CTC TCC TAT GTC AGC
	Major allele probe	cgc gcc gag gCG AAC CAG GGT TGA AT
	Minor allele probe	agg cca cgg acg TGA ACC AGG GTT GAA TT
	Invader oligo	CCA GGG AGC TCC CCG AAG GCG a

† Lowercase letters in each probe indicate 5'flap region.

therapy in Japanese (8), European (9), and a multi-ethnic population (10, 11). In particular, the two outstanding SNPs, rs12979860 and rs8099917 (located ~3 kb and 8 kb upstream of *IL28B*, respectively) have been found in strong association with the treatment response (8, 10). The minor allele frequency of rs8099917 was significantly higher in the null virological response (NVR) group compared with the virological response group. By taking advantage of *IL28B* typing, it may be possible to predict a NVR as well as a SVR in order to tailor the most suitable treatment regimens.

In this study, the "Invader Plus genotyping assay *IL28B* SNP" test kit including primers and probe setting was developed and compared with the usual TaqMan probe assay for genotyping *IL28B* SNPs and the pre-treatment prediction of the response to PEG-IFN-α/RBV therapy in HCV infection.

MATERIALS AND METHODS

Patients

DNA samples were obtained from 512 Japanese chronic hepatitis C patients, after informed consent, recruited from NHO Nagasaki Medical Center, Nagoya City University Hospital, Nagoya Daini Red Cross Hospital, and Kawasaki Medical University Hospital in Japan. Of them, the data of 90 patients were also used in a previous paper (15). All of the subjects had undergone a standard course of PEG-IFN-α/RBV therapy and 316 patients had their virological response status established before this study, of which 272 patients had HCV genotype 1. The NVR, transient virological response (TVR) and SVR were defined 24 weeks after PEG-IFN-α/RBV therapy, as previously described (8). This study classified the response outcome in two categories; responders (including those with SVR and TVR) and non-responders (including patients with NVR).

Informed consent was obtained from each patient and the study protocol 22 conformed to the ethics guidelines of the Declaration of Helsinki and was approved by 23 the institutional ethics review committee.

Samples for assay validation

To assess intra-assay and inter-assay precision and both coefficients of variation (CV%), three different genotype samples (major, minor, and hetero), two positive (major and minor) and one negative control were run in triplicate during three runs (three different days). The limit of detection was evaluated by analyzing three different genotype samples using two different DNA concentrations (1 ng, and 0.3 ng per assay) with the same three controls.

Invader Plus assay

The Invader Plus assay, which combines polymerase chain reaction (PCR) and the Invader reaction, was performed using the LC480II (Roche Diagnostics, Basel, Switzerland). The enzymes used in Invader Plus are native Taq polymerase (Promega, Fitchburg, WI, USA) and cleavase enzyme (Third Wave Technologies, Madison, WI, USA). Primers and allele probes newly designed for Invader Plus genotyping of *IL28B* SNPs are shown in Table 1 (Third Wave Japan, Tokyo, Japan). The reaction is configured to use PCR primers with a melting temperature (Tm) of 72°C and an Invader detection probe with a target-specific Tm of 63°C. The invader oligonucleotide overlaps the probe by one nucleotide, forming at 63°C an overlap flap substrate for the cleavase enzyme. The first step in Invader Plus is PCR target amplification, in which the reaction is subjected to 18 cycles of a denaturation step (95°C for 15 s) and hybridization and extension steps (70°C for 1 min). At the end of PCR cycling, the reaction mixture is

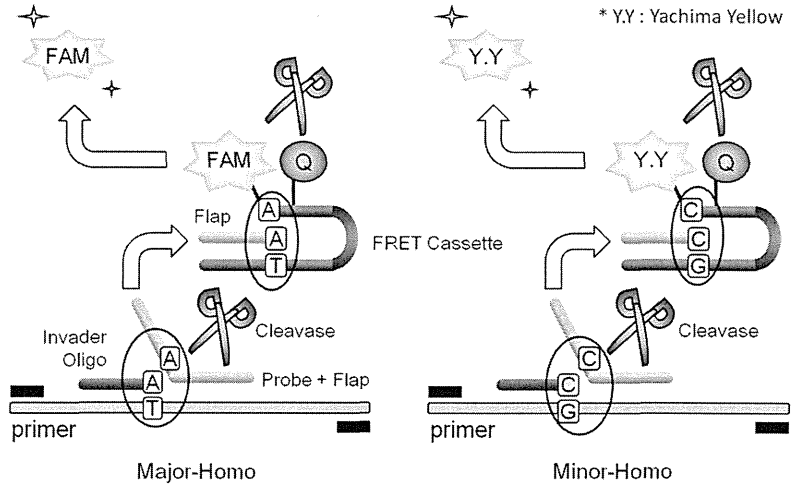

Fig. 1. Principle of the Invader Plus genotyping assay for *IL28B* single nucleotide polymorphisms (SNPs) (for rs8099917). First, an Invader Oligo and a probe are annealed to amplified target DNA, overlapping at the SNP position, which clipped out the 5'flap fragment by the cleavase enzyme. Second, the released 5'flapanneals to the fluorescence resonance energy transfer (FRET) cassette and initiates a secondary cleavage reaction that releases the fluorescent dye. The signal is only released when the invasive structure is formed on the target DNA. 'Major allele' is left FAM signal, 'Minor allele' is right Yackima-Yellow (Y.Y) signal, and 'Hetero-type' observed both merged signals, respectively. The fluorescent dye is between major and minor alleles at rs12979860.

incubated at 99°C for 10 min to inactivate the Taq polymerase. Next, the reaction temperature is lowered to 63°C for 15 min to permit hybridization of the probe oligonucleotide and formation of the overlap flap structure (Fig. 1). Data were analyzed by endpoint genotyping software (Roche Diagnostics).

TaqMan PCR assay

The rs8099917 polymorphism was determined using TaqMan Pre-Designed SNP Genotyping Assays, as recommended by the manufacturer (Life Technologies, Carlsbad, CA, USA). The Custom TaqMan SNP Genotyping Assay Service MGB probe was used to determine the genotype of rs12979860 (Life Technologies). Each genome DNA sample (10 ng) was amplified using the master mix reagent of LightCycler480 Probe Master (Roche Diagnostics). The assays were carried out using the LC480II under the following conditions: 2 min at 50°C, 10 min at 95°C, 40 cycles: 15 s at 95°C, and 1 min at 60°C. Data were analyzed by endpoint genotyping software (Roche Diagnostics).

Direct sequencing assay

Before proceeding to *IL28B* SNP genotyping by the two methods, 105 DNA samples were genotyped using direct sequencing. To determine the SNP genotype of rs8099917 and rs12979860, the specific primer sets, rs8099917F (5'-AAGTAACACTTGTTCCTTRTAAAAGATTCC-3') and rs8099917R (5'-CGCTATAATTAAAGATGTGGGAGAA-TGCAA-3'), rs12979860F (5'-CACGGTCGTGCCTGTC-GTGT-3') and rs12979860R (5'-TGTGCTGTGCCTTCA CGCTCCGAGCA-3') were used, respectively (Life Technologies). The amplification products were sequenced directly in both forward and reverse directions with Prism Big Dye (Life Technologies) on an ABI3100 DNA automated sequencer (Life Technologies).

RESULTS

Assay validation

In this study, the performance characteristics of the assay were determined before experimental testing. To assess the accuracy of *IL28B* SNP genotyping based on both rs8099917 and rs12979860, the results from the Invader Plus genotyping assay were compared with the results from direct sequencing. Of the 105 DNA samples, 70 samples had the major homozygous allele, 30 samples the minor heterozygous and five samples the minor homozygous allele for both SNPs by direct sequencing. This gave 100% concordant results for rs12979860 between the two assays, although one sample showed different results for rs8099917 with direct sequencing. As a result of direct sequencing, this sample had the major homozygous allele, but the results of the Invader assay and TaqMan assay both showed the minor heterozygous allele. Precision was determined by analyzing six samples (including positive and negative controls) in triplicate during three runs (three different days) with 100% concordant results. Intra-assay coefficient of variation (CV%) for rs8099917 was 0.1–1.6 (%), and for rs12979860 was 0.5–2.5 (%). Then, inter-assay CV% calculated from the angle of the heterozygous allele marker was 1.9 and 2.0 (%), respectively (Fig. 2 and Table 2). To evaluate the limit of detection, 10 samples, including three genotypes, were run in triplicate using three different DNA concentrations with no visible confusion in *IL28B* SNP genotyping or signal intensity, except in the 0.3 ng/assay (Fig. 3).

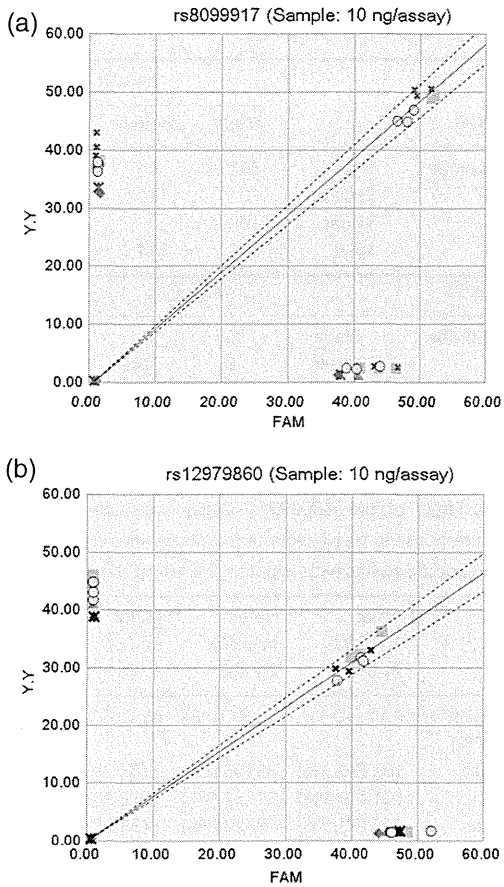

Fig. 2. Simultaneous and daily repeatability of Invader Plus genotyping assay for *IL28B* single nucleotide polymorphisms (SNPs) (three times per day and 3 days of measurement). Scatter plots of fluorescence data from intra-assay for rs8099917 (a) and for rs12979860 (b). Raw fluorescence data are plotted for each sample and control. The x-axis of rs8099917 is the FAM, corresponding to the major allele, while y-axis is Yachima-Yellow (Y.Y), corresponding to the minor allele. In contrast, the x-axis FAM and y-axis Y.Y of rs12979860 signify minor and major alleles, respectively. The line designates the mean of the angle at the heterozygous allele marker, and the broken line indicates standard deviation +2SD and −2SD. Day 1, control (♦); day 1, sample (■); day 2, control (▲); day 2, sample (×); day 3, control (×); day 3, sample (○); mean (—); +2SD (---); −2SD (---).

IL28B typing in PEG-IFN-α/RBV-treated patients

Of the 512 cases that were analyzed for the rs8099917 genotype, 361 (71%) were shown to have a major homozygous allele, 144 (28%) had a minor heterozygous, and seven (1%) had a minor homozygous allele, which gave concordant results with the TaqMan assay (Table 3). In addition, of the 512 cases that were analyzed for the rs12979860 genotype, 356 (70%) were shown to have a major homozygous allele, 149 (29%) had a minor heterozygous, and seven (1%) had a minor homozygous allele, with 100% concordant results with the TaqMan assay (Table 3). Five of the 512 cases (1%) had haplotype differences, but none of the 512 cases showed differences between the two genotyping methods.

Table 2. Simultaneous and daily repeatability of Invader Plus genotyping assay for *IL28B* single nucleotide polymorphisms (SNPs) (three times per day and 3 days of measurement)

		Coefficient of variation (%)	
		rs8099917	rs12979860
Hetero (10 ng/assay)	Day1	0.1	1.4
	Day2	1.6	2.5
	Day3	1.3	0.5
	Total	1.9	2.0

Prediction of a response to PEG-IFN-α/RBV therapy

Of the 272 patients with genotype 1 who were evaluated for the treatment response, 169 of 203 patients with the major homozygous allele in rs8099917 exhibited a higher prevalence of a virological response (83.3%), consisting of a SVR and TVR (responder), compared with those with a minor heterozygous (18/66, 27.3%) or homozygous allele (1/3, 33.3%) (Table 4). Therefore, the prevalence of responders with the major homozygous allele was 83.3%, and that of non-responders with the minor heterozygous or homozygous allele was 72.5%. Of the 36 patients with genotype 2a or 2b, patients with a major homozygous allele had 96.7% incidence of virological response and those with a heterozygous allele had 100%. For all cases, 85.2% of the patients with a major homozygous allele were responders to PEG-IFN-α/RBV therapy, and 66.7% of the patients with a minor heterozygous or homozygous allele were non-responders to that therapy.

DISCUSSION

The rate of a NVR after 48 weeks of PEG-IFN-α/RBV therapy among patients infected with HCV genotype 1 is around 20–30%. Previously, there have been no reliable predictors of a NVR or SVR. Some recent studies have focused on the *IL28B* polymorphism as one of the most critical factors with a bearing on the prediction of the treatment response (8–10). In particular, rs8099917 and rs12979860 were significantly associated with the treatment regimen; therefore, it would be useful to examine such genetic markers before IFN-based treatments in clinical practice because it would avoid the unpleasant side effects that commonly accompany the treatment. In addition, such an advanced diagnosis would be economically beneficial, as treatment costs would be reduced.

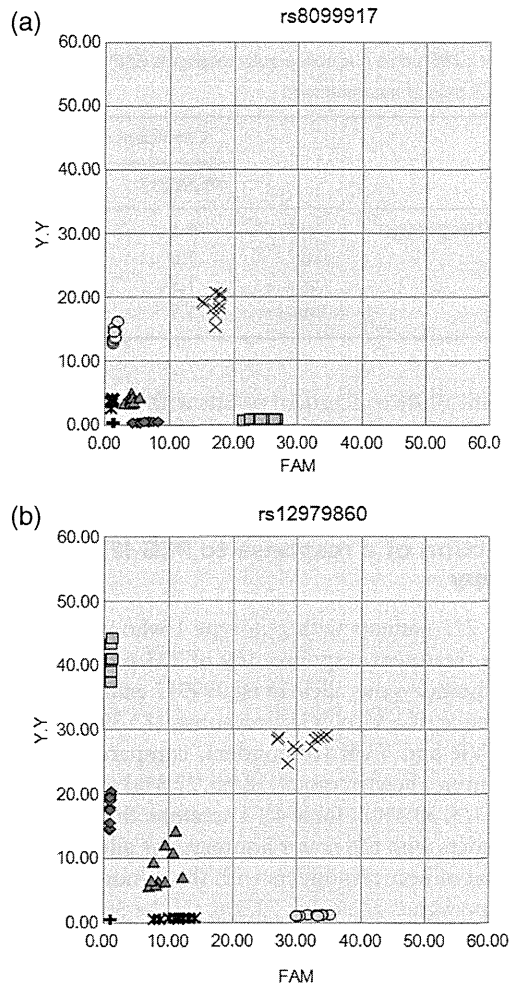

Fig. 3. Sensitivity of Invader Plus genotyping assay for *IL28B* single nucleotide polymorphisms (SNPs). Scatter plots of fluorescence data from intra-assay for rs8099917 (a) and for rs12979860 (b). It was defined that the major allele is "Major", hetero type is "Hetero", the minor allele is "Minor", and Negative control is "Neg", respectively. Major (0.3 ng) (◆); major (1.0 ng) (⧈); hetero (0.3 ng) (▲); hetero (1.0 ng) (×); minor (0.3 ng) (✱); minor (0.3 ng) (○); + Neg (+).

Some SNPs, such as UGT1A1 polymorphism associated with irinotecan therapy, have already been exploited in clinical practice to avoid severe adverse effects (12, 13). These tailor-made therapies are expected to become more common in clinical practice (14). Similarly, *IL28B* polymorphism detection can be used in tailor-made therapies; thus, it is important to develop a genotyping assay that is convenient, swift, accurate, and inexpensive.

The Invader Plus genotyping assay *IL28B* SNP test kit to genotype *IL28B* SNPs (rs8099917 and rs12979860) from DNA samples was developed and evaluated in this study. This assay contains reagents for DNA amplification, including each SNP. Accuracy was determined by comparing the Invader assay results with the direct sequencing results. Only one sample (0.95%) showed a discrepant result for rs8099917 by comparing the Invader Plus genotyping assay and direct sequencing, because another rare SNPs existed in the forward primer binding region used for amplification and direct sequencing (15). Intra-assay (0.1–1.6% for rs8099917 and 0.5–2.5% for rs12979860) and inter-assay (1.9 and 2.0% respectively) precision were sufficient for clinical practice and tailor-made therapies. Interestingly, Invader Plus assay is more convenient, swift and inexpensive than direct sequencing. Invader Plus assay is better than TaqMan assay at specificity because no results come up without tagging both probe and Invader oligonucleotide on SNP directly.

For each or both genotypes, influences on pretreatment prediction with the *IL28B* SNP genotype were evaluated. As a result, especially for patients with genotype 1b, the positive predictive value (PPV) for a NVR was 72.5% and the negative predictive value (NPV) was 83.3%, suggesting that a convenient method using the Invader Plus assay could be useful to predict the treatment outcome in clinical practice.

Table 3. Comparisons of the Invader Plus genotyping assay with TaqMan assay for rs8099917 and rs12979860

		Invader Plus			
rs8099917		Major	Hetero	Minor	total
TaqMan probe	Major	361	0	0	361
	Hetero	0	144	0	144
	Minor	0	0	7	7
	total	361	144	7	512
rs12979860		Invader Plus			
TaqMan probe	Major	356	0	0	356
	Hetero	0	149	0	149
	Minor	0	0	7	7
	total	356	149	7	512

Table 4. Effect of the rs8099917 single nucleotide polymorphisms (SNPs)on response to pegylated interferon/ ribavirin (PEG-IFN/RBV) therapy in Japanese patients with hepatitis C virus (HCV) genotype 1

	Major ($n=203$) 74.6%	Hetero ($n=66$) 24.3%	Minor ($n=3$) 1.1%	Total ($n=272$)
Mean age (SD)	57.2 (10.1)	54.9 (10.8)	65.7 (6.5)	56.7 (10.3)
Gender (%)				
Females	102 (50.2%)	35 (53.0%)	2 (66.7%)	139 (51.1%)
Males	101 (49.8%)	31 (47.0%)	1 (33.3%)	133 (48.9%)
Responder	169 (83.3%)	18 (27.3%)	1 (33.3%)	188 (69.1%)
Non-responder	34 (16.7%)	48 (72.7%)	2 (66.7%)	84 (30.9%)